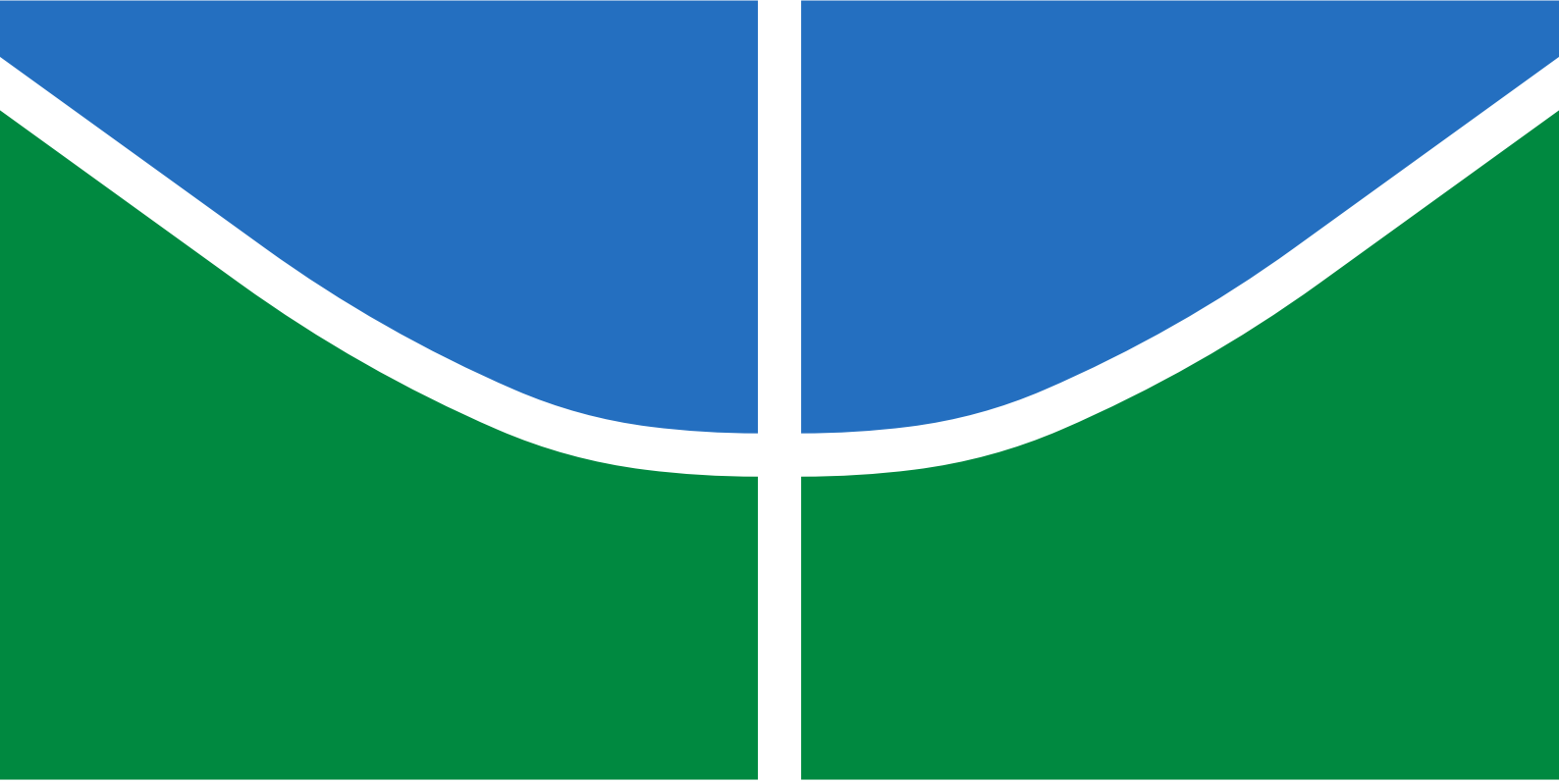

Array Interpolation Methods with applications in Wireless Sensor Networks and Global Positioning Systems

Marco Antonio Marques Marinho

DISSERTAÇÃO DE MESTRADO EM ENGENHARIA ELÉTRICA

DEPARTAMENTO DE ENGENHARIA ELÉTRICA

Brasília, Dezembro de 2013

FACULDADE DE TECNOLOGIA

UNIVERSIDADE DE BRASÍLIA

UNIVERSIDADE DE BRASÍLIA
FACULDADE DE TECNOLOGIA
DEPARTAMENTO DE ENGENHARIA ELÉTRICA

Array Interpolation Methods with applications in Wireless Sensor Networks and Global Positioning Systems

Marco Antonio Marques Marinho

ORIENTADOR: João Paulo Carvalho Lustosa da Costa
COORIENTADOR: Felix Antreich

DISSERTAÇÃO DE MESTRADO EM ENGENHARIA ELÉTRICA

PUBLICAÇÃO: PPGEE.DM - 547/2013
BRASÍLIA/DF: DEZEMBRO - 2013

UNIVERSIDADE DE BRASILIA
Faculdade de Tecnologia
Mestrado em Engenharia Elétrica

DISSERTAÇÃO DE MESTRADO EM ENGENHARIA ELÉTRICA
DEPARTAMENTO DE ENGENHARIA ELÉTRICA

Array Interpolation Methods with applications in Wireless Sensor Networks and Global Positioning Systems

Marco Antonio Marques Marinho

Relatório submetido como requisito parcial de obtenção de grau de Mestre em Engenharia Elétrica

Banca Examinadora

Prof. Dr.-Ing. João Paulo Carvalho Lustosa da Costa, UnB
Orientador _____

Dr.-Ing. Felix Antreich, DLR
Coorientador _____

Prof. Dr. Edison Pignaton de Freitas, UFSM
Examinador externo _____

Prof. Dr. Rafael Timóteo de Sousa Júnior, UnB
Examinador interno _____

Brasília, Dezembro de 2013

FICHA CATALOGRÁFICA

MARINHO, MARCO ANTONIO MARQUES
Array Interpolation Methods with applications in Wireless Sensor Networks and Global Positioning Systems [Distrito Federal] 2013.

viii, 62p., 297 mm (ENE/FT/UnB, Mestre, 2013) Dissertação de Mestrado – Universidade de Brasília. Faculdade de Tecnologia.

1. Arranjos de Antenas
2.Interpolação de Arranjos
3. Sistemas de Posicionamento Global
4.Redes de Sensores

I. ENE/FT/UnB
II. Título (série)

REFERÊNCIA BIBLIOGRÁFICA

MARINHO, M. A. M., (2013). Array Interpolation Methods with applications in Wireless Sensor Networks and Global Positioning Systems, Dissertação de Mestrado em Engenharia Elétrica, Publicação PPGEE.DM-547/2013, Departamento de Engenharia Elétrica, Universidade de Brasília, Brasília, DF, 62p.

CESSÃO DE DIREITOS

AUTOR: Marco Antonio Marques Marinho

TÍTULO: Array Interpolation Methods with applications in Wireless Sensor Networks and Global Positioning Systems

GRAU: Mestre ANO: 2013

Marco Antonio Marques Marinho

SMPW Quadra 16 Conjunto 04 Lote 11 Casa H

71.741-604 Brasília – DF – Brasil.

Dedicatória

Aos meus pais:
Marco Antonio e Marcelita, tudo que conquistei e conquistarei só é possível graças ao seu amor incondicional e sacrifício.

Ao meu irmão:
Murilo, meu grande exemplo e razão pela qual hoje sou pesquisador.

Marco Antonio Marques Marinho

Agradecimentos

A Deus por me iluminar a abençoar durante todo meu trajeto nessa vida.

Devo muito ao meu orientador Professor João Paulo Carvalho Lustosa da Costa pela oportunidade de trabalhar sobre sua excelente tutela, pela confiança e enorme oportunidade ao me indicar para a Agência Espacial Alemã, pela paciência ao longo de longas discussões, pelo grande apoio e incentivo e, acima de tudo, por ter me ensinado a possuir grande respeito e admiração pelo campo de processamento de sinais em arranjos. Trabalhar ao seu lado tem sido uma experiência incrivelmente recompensadora e espero que essa parceria dure por um longo tempo.

Um agradecimento especial ao meu coorientador na Alemanha, Felix Antreich, por tornar a Agência Espacial Alemã minha segunda casa, pela enorme paciência inicial nas primeiras explicações e discussões sobre os sistemas GPS, por confiar no meu potencial ao me convidar e ao me repassar um problema relevante, pela ajuda imensurável com todo e qualquer problema que tive durante minha estada na Alemanha e por me apontar a área de interpolação de arranjos onde conduzo pesquisa com grande satisfação e interesse. Levarei sempre comigo sua capacidade incrível de sorrir a qualquer momento e de gerar entusiasmo em todos ao seu redor.

Ao Professor Edison Pignaton de Freitas pela paciência, pelo constante incentivo, pela confiança e oportunidade de contribuir em nossa pesquisa conjunta na área de redes de sensores, pesquisa que persigo com enorme prazer e entusiasmos, pela disponibilidade e pelo incansável acompanhamento e apoio nos trabalhos, por todas as correções e sugestões que me permitiram evoluir e buscar sempre padrões mais altos em meus trabalhos. Espero que juntos possamos contribuir muito ainda para a área de redes de sensores.

Ao Professor Rafael Timóteo de Sousa Júnior por contribuir imensamente com o curso de Engenharia de Redes na Universidade de Brasília, pela competência científica, pela paciência, pela disponibilidade manifestada e pelo apoio prestado para a publicação de inúmeros trabalhos.

Aos membros da secretaria do ENE, em especial a Ana Carolina e Adriana por sua disponibilidade e capacidade incrível de resolver problemas burocráticos mesmo durante minha ausência. Sem vocês provavelmente não conseguiria o titulo de mestre.

Marco Antonio Marques Marinho

RESUMO

Array Interpolation Methods with applications in Wireless Sensor Networks and Global Positioning Systems

Autor: Marco Antonio Marques Marinho

Orientador: João Paulo Carvalho Lustosa da Costa

Coorientador: Felix Antreich

Programa de Pós-graduação em Engenharia Elétrica

Brasília, Dezembro de 2013

Nas últimas três décadas o estudo de técnicas de processamento de sinais em arranjos de sensores tem recebido grande atenção. Uma grande quantidade de técnicas foi desenvolvida com diversas finalidades como a estimação da direção de chegada, a filtragem ou separação espacial dos sinais recebidos, a estimação do atraso de propagação, a estimação da frequência Doppler e a pré-codificação de sinais na transmissão para maximização da potência recebida por outro arranjo. Técnicas para estimação da direção de chegada são de particular interesse para sistemas de posicionamento baseado em ondas de rádio, como os sistemas de posicionamento global e para o mapeamento de sensores em redes de sensores. Uma particularidade dessas aplicações é a necessidade de uma estimação em tempo real ou computacionalmente eficiente. Técnicas de estimação da direção de chegada que atendem esses requisitos requerem uma estrutura muito específica do arranjo de antenas que, em geral, não pode ser obtida em implementações reais. Nesse trabalho é apresentado um conjunto de técnicas que permitem a interpolação de sinais recebidos em arranjos de geometria arbitrária para arranjos de geometria específica, de forma eficiente e robusta, para possibilitar a aplicação de técnicas eficientes para estimação da direção de chegada em arranjos de geometria arbitrária. Como aplicações das técnicas propostas são apresentados o mapeamento preciso em redes de sensores e posicionamento preciso em receptores de sistemas de posicionamento global.

Palavras Chave: Arranjos de Antenas, Interpolação de Arranjos, Redes de Sensores, Sistema de Posicionamento Global

ABSTRACT

Array Interpolation Methods with applications in Wireless Sensor Networks and Global Positioning Systems

Author: Marco Antonio Marques Marinho

Supervisor: João Paulo Carvalho Lustosa da Costa

Co-supervisor: Felix Antreich

Programa de Pós-graduação em Engenharia Elétrica

Brasília, December of 2013

In the last three decades the study of antenna array signal processing techniques has received significant attention. A large number of techniques have been developed with different purposes such as the estimation of the direction of arrival (DOA), filtering or spatial separation of received signals, estimation of time delay of arrival (TDOA), Doppler frequency estimation and precoding of transmitted signals to maximize the power received by a different array. DOA estimation techniques are of particular interest for positioning systems based on radio waves such as the global positioning system (GPS) and for sensor mapping in wireless sensor networks (WSNs). These applications have the particular requirement of demanding the estimations to be made in real time or with reduced computational complexity. DOA estimation techniques that fulfill these requirements demand very specific antenna array structures that cannot, in general, be obtained in real implementations. In this work a set of techniques is presented that allows the interpolation of signals received in arrays of arbitrary geometry into arrays of specific geometry efficiently and robustly to allow the application of efficient DOA estimation techniques in arrays of arbitrary geometry. As an application of the proposed techniques precise mapping for WSNs and precise positioning for GPS receivers is presented.

Keywords: Antenna Arrays, Array Interpolation, Wireless Sensor Networks, Global Positioning Systems

CONTENTS

LIST OF FIGURES

LIST OF TABLES

LIST OF SYMBOLS

$\otimes$	Kronecker product
$\odot$	Hadamard-Schur product
$\diamond$	Khatri-Rao product
*	Complex conjugate
$^{\mathrm{T}}$	Transpose of a matrix
$^{\mathrm{H}}$	Complex conjugate transpose of a matrix
†	Matrix Pseudoinverse
$\lceil \cdot \rfloor_{\mathcal{D}}$	Rounding operation unto a discrete domain $\mathcal{D}$
eig	Eigenvalues of a matrix
j	Complex unity

Capítulo 1

Sumário

Processamento de sinais em arranjos tem sido o foco de grande atenção pela comunidade científica nas últimas três décadas. Organizando os dados obtidos por um conjunto de sensores e aplicando conceitos da matemáticos e estatísticos pode-se extrair uma vasta gama de informações do sinais medidos. Um dos pontos de maior interesse no processamento de sinais em arranjos é a estimação de parâmetros. No contexto de arranjos de antenas entende-se por parâmetro a direção de chegada, o atraso de propagação ou a frequência Doppler de um sinal. Todos esses parâmetros podem ser estimados utilizando-se arranjos de antenas juntamente de algum conhecimento prévio como a geometria do arranjo ou a resposta do arranjo à diferentes tipos de sinais.

Estimação da direção de chegada

Entre todos os parâmetros que podem ser estimados a estimação da direção de chegada é de grande interesse e tem recebido atenção especial no campo de processamento de sinais. Uma vez que o receptor possui conhecimento sobre a direção de chegada dos sinais um filtro espacial pode ser aplicado, separando efetivamente o sinal recebido de uma direção dos sinais recebidos em todas as outras. A direção de chegada é um dos parâmetros fundamentais em sistemas de radar, como o sistema de radio altímetro preciso proposto em [1], e também em situações de guerra eletrônica. Uma aplicação futura relevante da estimação da direção de chegada é a navegação precisa de veículos aéreos não tripulados como pode ser visto em [2].

O problema da estimação da direção de chegada de sinais em um arranjo de antenas está exemplificado na Figura 1.1. O arranjo mostrado na figura é conhecido como um arranjo linear uniforme e possui a propriedade muito interessante de que para uma determinada direção de chegada existe uma diferença de fase exata e única no sinal recebido entre duas antenas adjacentes. Portanto, para esse tipo de arranjo, havendo apenas um sinal, a direção de chegada do sinal pode ser estimada observando-se apenas essa diferença de fase. Até quando há mais de um sinal incidente o arranjo uniforme ainda oferece um grande número de vantagens e, portanto, é o tipo de arranjo assumido na maioria dos trabalhos de estimação de direção de chegada da literatura.

Apesar da existência de métodos que permitem a estimação de parâmetros em arranjos com

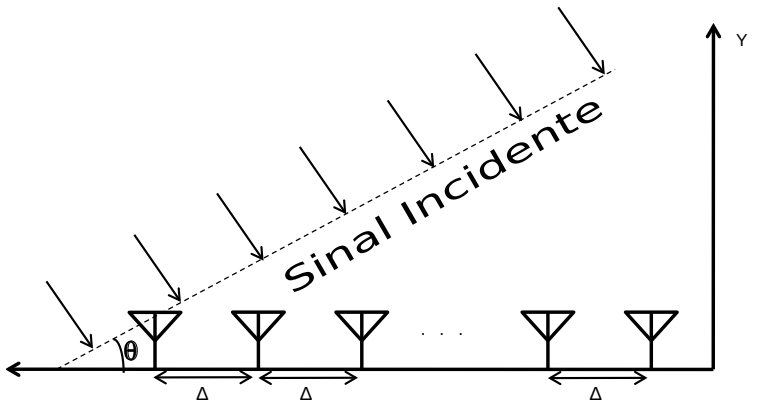

Figure 1.1: Sinal incidindo sobre um arranjo de antenas e sua respectiva direção de chegada

Família	Métodos
Máxima Verosimilhança	Máxima Verosimilhança clássica EM SAGE IQML
Beamformers	Beamformer clássico CAPON-MVDR
Métodos de Subespaço	MUSIC Root-MUSIC ESPRIT Root-WSF

Table 1.1: Sumário de métodos de estimação de direção de chegada

qualquer tipo de geometria, como os métodos de Máxima Verosimilhança (ML) [3, 4] e suas derivações: Esperança-Maximização (EM) [5, 6, 7, 8] e o Esperança-Maximização Alternando no Espaço (SAGE) [9, 10]. Esses métodos são iterativos e tem grandes custos computacionais e suas extensões EM e SAGE, apesar de garantirem uma carga computacional mais baixa, não garantem a convergência para um máximo global [11] e requerem que o receptor tenha conhecimento da quantidade de sinais recebidos. Diferentemente do conceito ML, a família de métodos conhecida como beamformer usa a soma de forma construtiva ou destrutiva de sinais para estimar a direção de chegada dos sinais. Entre esses métodos se destacam os apresentados em [12, 13]. Mais recentemente a comunidade científica tem dedicado muita atenção aos métodos baseados em subespaço. Esses métodos utilizam os conceitos da estatística de decomposição de dados em componentes principais para separar os dados recebidos em uma parte que representa a estatística dos sinais e outra que representa a estatística do ruído. Esses métodos são extremamente eficientes em termos computacionais e apresentam um excelente desempenho mesmo na presença de forte ruído. Um ponto

negativo desses métodos, entretanto, é a incapacidade de lidar com sinais que possuam uma forte correlação, já que a separação estatística assume que os sinais sejam descorrelacionados. Felizmente, existem na literatura alternativas capazes de descorrelacionar os sinais recebidos no arranjo [14] e [15]. Infelizmente essas técnicas requerem um arranjo com uma geometria extremamente específica que nem sempre pode ser construída em implementações reais e também sacrificam a resolução do arranjo.

Interpolação de Arranjos

Para lidar com essa limitação na construção de arranjos com geometrias extremamente precisas ou respostas difíceis de serem obtidas a técnica de interpolação de resposta foi desenvolvida [16, 17, 18, 19]. Com essa técnica é possível mapear os dados recebidos em qualquer arranjo para o que seria recebido em um arranjo com uma estrutura especifica e precisa usando um matriz de transformação **B** como mostra a Figura 1.2.

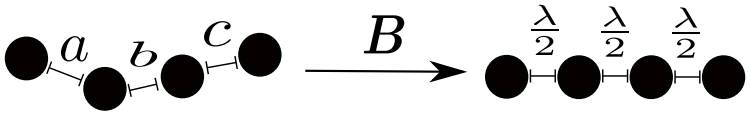

Figure 1.2: Representação gráfica da matrix de transformação

As técnicas de interpolação presentes hoje na literatura dividem o campo de resposta do arranjo em várias regiões, chamadas setores, e aplicam uma interpolação seguida de uma estimação de parâmetros para cada setor. Após a transformação para o arranjo virtual desejado as técnicas para a descorrelação de sinais são aplicadas [16] e algoritmos para a estimação da direção de chegada como o Root-MUSIC podem ser aplicados [17]. O cálculo das matrizes de transformação precisa ser muito cuidadoso de forma a minimizar o erro induzido pela transformação e ao mesmo tempo controlar a resposta de sinais fora do setor transformado. Os primeiros trabalhos de interpolação de arranjos ignoraram a resposta de sinais fora do setor [16, 17, 18, 19]. Outro problema da interpolação de arranjos é que, mesmo se o ruído for descorrelacionado na entrada, a interpolação promove a correlação do ruído. Portanto, um passo de descorrelação do ruído é necessário para a aplicação das técnicas de subespaço como o MUSIC [20] e Root-MUSIC [21, 17]. Essa descorrelação de ruído destrói a invariância rotacional necessária para o ESPRIT [22]. Trabalhos mais recentes como foco em sinais correlacionados propuseram o controle dos sinais fora do setor por meio de uma penalização adaptativa ao sinal recebido [23],[24].

A abordagem atual setor a setor usada para a interpolação de arranjos para a estimação da direção de chegada resulta em alguns problemas;

- Não há garantia sobre o comportamento dos sinais fora do setor, o que pode levar a imprecisões na estimação. Transformar todo o campo de resposta do arranjo por outro lado também resulta em grandes imprecisões.
- Estimar o numero de sinais se torna problemático. Os sinais fora do setor devem ser consi-

derados ou não?

- A escolha entre diferentes estimativas de setores distintos não é simples. Como decidir se duas estimativas pertencem ao mesmo sinal ou a sinais distintos?
- Como a transformação se comporta quando o conhecimento sobre a resposta verdadeira do arranjo ou sobre sua verdadeira geometria é limitado?

Interpolação de Arranjos Proposta

Neste trabalho é proposta uma abordagem que se adapta ao sinal recebido para tratar os problemas mencionados. A abordagem proposta pode ser dividida em oito passos como mostra a Figura 1.3. A área indicada pela linha tracejada se refere aos passos necessários para o cálculo de uma transformação ideal para resolver os problemas citados e o foco desse trabalho.

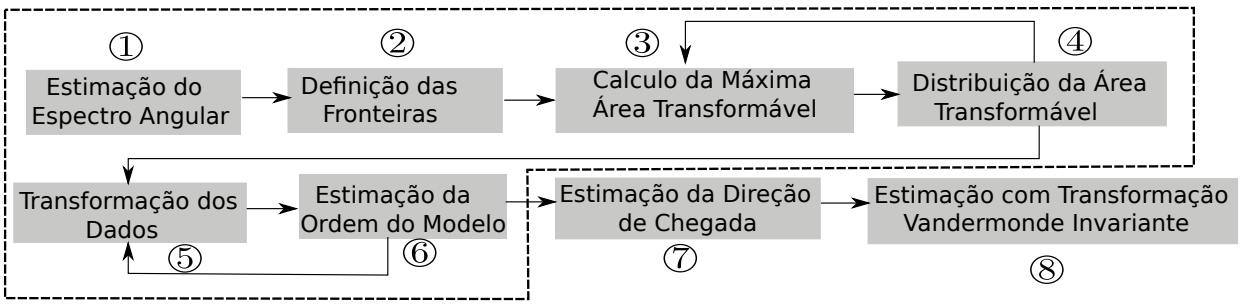

Figure 1.3: Diagrama da abordagem proposta

São as seguintes as características fundamentais definidas na proposta aqui tratada:

- Em ①, para evitar o processamento clássico setor a setor, uma primeira estimativa não muito precisa das regiões angulares do arranjo que recebem potência significativa é obtida. Essa estimação é um processo muito simples e de baixa demanda computacional.
- Em ②, os resultados do primeiro passo são usados para decidir quais regiões angulares do arranjo valem a pena ser transformadas e quais regiões contêm apenas ruído e podem ser ignoradas. Esse passo também possui um baixo custo computacional.
- Em ③ e ④ o resultado de ② é utilizado para decidir como melhor aplicar a transformação sobre as regiões detectadas. Esse passo procura garantir que a transformação não introduza grandes erros na estimação final das direções de chegada enquanto, ao mesmo tempo, tenta garantir que a menor potência possível de sinal seja deixada de fora da transformação.
- Em ⑤ e ⑥, uma transformação que leva em consideração o ruído recebido sobre o arranjo é obtida e o sinal original recebido é transformado aplicando simultaneamente técnicas de descorrelação de sinais. Esse passo é executado em paralelo com a estimação do número de sinais de forma a garantir que todos os sinais sejam efetivamente separados sem sacrificar

gravemente a resolução do arranjo. Esse passo resolve o problema de estimação de sinais presente nos métodos anteriores já que nenhum sinal foi deixado de fora da transformação.

- Em ⑦, a direção de chegada de todos os sinais é estimada simultaneamente usando-se o ESPRIT. Esse passo resolve muitos problemas apontados nas abordagens anteriores. Já que todos os sinais são estimados simultaneamente, não há necessidade de escolher quais estimativas são reais ou escolher entre diferentes estimativas. Só há uma estimativa para cada sinal e todas são reais.
- Por último, em ⑧ uma segunda transformação é empregada para obter resultados ainda mais precisos. Infelizmente essa precisão extra tem o custo de uma complexidade computacional adicional. Esse passo, porém, é opcional e pode ser usado, por exemplo, em sistemas com grande capacidade computacional.

Aplicações

De forma a demonstrar a flexibilidade e versatilidade do método proposto são apresentadas duas aplicações. A primeira é um receptor para sistemas de navegação global baseado em arranjos de antenas. Esses sistemas sofrem com a presença de sinais fortemente correlacionados que podem ser componentes de multipercurso de um satélite ou sinais interferentes emitidos por um adversário. A segunda aplicação pressupõe de uma rede de sensores que foram lançados aleatoriamente em um espaço e consiste na transformação de uma rede de sensores em um arranjo de antenas plenamente funcional.

Receptor para Sistemas de Posicionamento Global Usando Arranjos de Antenas

Na aplicação referente a sistemas de posionamento global, o objetivo é estimar o atraso de propagação do sinal de linha de visada entre o satélite e o receptor. Para isso apresenta-se o sistema proposto na Figura 1.4.

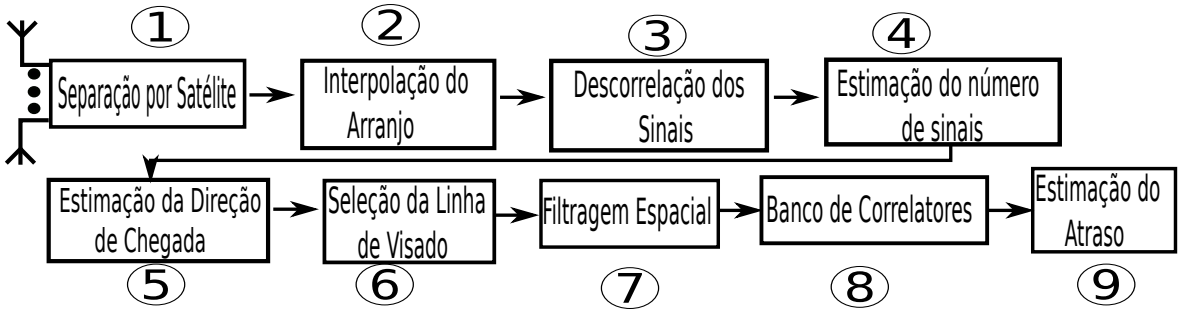

Figura 1.4: Diagrama de blocos do sistema proposto - Receptor GPS

Em ① os dados recebidos dos múltiplos satélites são separados usando a propriedade da transmição com códigos ortogonais dos sistemas de navegação global. Esse passo é extremamente importante já que reduz drasticamente o número de antenas necessárias no receptor.

Em ②, ③, ④ e ⑤ a proposta de interpolação de arranjos para estimação de direção de chegada desse trabalho é aplicada.

Em ⑥ a componente referente a linha de visada do satélite é selecionada. Esse passo descarta sinais interferentes adversários, uma realidade, por exemplo, em aplicações militares.

Em ⑦, usando a direção de chegada estimada pode-se aplicar um filtro espacial para selecionar apenas a componente de linha de visada. Essa separação é muito importante para a estimação do atraso.

Em ⑧ é aplicado um banco de correlatores que se comporta como um arranjo de antenas no tempo ao invés do espaço. Isso permite a aplicação de métodos de estimação de direção de chegada, como o MUSIC, para a estimação do atraso do componente de linha de visada do satélite.

Por último, em ⑨ um método de estimação de direção de chegada de alta resolução, o MUSIC, é aplicado para estimar o atraso com precisão.

Redes de Sensores Como Arranjos de Antenas

Na aplicação para redes de sensores é apresentado um método simples para o mapeamento interno da rede. Esse método não requer a presença de nenhum agente externo, como um sinal do sistema de posicionamento global, e requer apenas a presença de uma antena de dipolo cruzado em cada sensor. Esse arranjo pode ser usado, por exemplo, para filtrar sinais interferentes que venham de fora da rede de sensores. A implementação, tanto do hardware quanto do software, do método proposto é extremamente simples o que permite a sua aplicação no contexto de redes de sensores. As localizações mapeadas são usadas para a aplicação a técnica de interpolação de arranjos proposta. A rede de sensores é efetivamente transformada em um arranjo de antenas completamente funcional como exemplificado na Figura 1.5.

Figura 1.5: Interpolação de uma rede de sensores para um arranjo de antenas

Validação

Para validar a técnica proposta um conjunto de simulações numéricas é apresentado. O desempenho da estimação de direção de chegada é comparado com o método proposto em [24]. O método proposto em [24] controla a resposta da região fora do setor transformando todo o arranjo. Isso resulta em um grande erro de transformação que não tem relação com o nível de ruído recebido, e,

portanto, este método tem uma performance que é limitada pela própria transformação. Já o método proposto neste trabalho tem uma performance superior e um erro menor conforme a relação sinal ruído melhora. Graças ao passo de análise do espectro espacial, que se torna melhor definido conforme o ruído diminui, a área do arranjo que é transformada diminui conforme a relação sinal ruído cresce. Isso resultado em um resultado mais preciso e um erro que decresce conforme o ruído diminui.

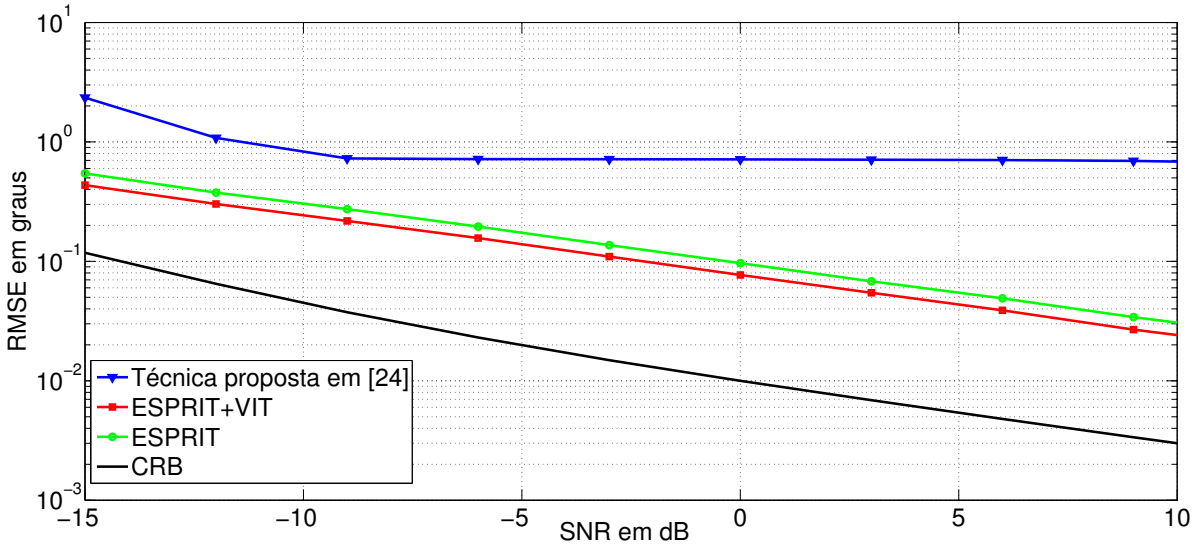

Figure 1.6: RMSE de [24] e técnica proposta com e sem o passo VIT

Contribuições

Este trabalho apresenta como principal contribuição um novo método para a interpolação de arranjos com uma performance superior as técnicas presentes atualmente na literature. O método proposto evita inúmeros problemas que são ignorados pelas técnicas que existem atualmente, como a estimação de sinais fantasmas, sinais que não existem realmente. O método também trata de problemas que são ignorados atualmente, como a estimação do número de sinais presente no arranjo após a transformação do arranjo.

O método de interpolação é aplicado para o desenvolvimento de um receptor de sistemas de posicionamento global preciso e capaz de lidar com a presença de sinais fortemente correlacionados que normalmente degradariam fortemente a precisão desses sistemas. Além disso o método é aplicado a redes de sensores para transformar uma rede de sensores em um arranjo de antenas totalmente funcional, transformando a rede de sensores em um sistema extremamente robusto e versátil.

Chapter 2

Introduction

Antenna array signal processing has been the focus of many researches in the last three decades, a subfield of particular interest is parameter estimation using antenna arrays. High resolution signal processing using antenna arrays borrows its concepts from linear algebra, specially due to the EVD used in most methods, in order to achieve improved results and break from the traditional Fourier analysis point of view and its inherent limitations. In the antenna array field the parameters to be estimated are those related to the received wave signals, spatial parameters such as direction of arrival (DOA) and direction of departure (DOD), temporal parameters such as time delay of arrival (TDOA) and frequency parameters such as Doppler shift all can be estimated by fusing together the data received at various antennas and using a preexisting knowledge such as the geometry in which the antennas are organized and their responses to signals arriving with different center frequencies or from different directions. Concepts of antenna array signal processing can even be extended to ensure longer lifetime and better connectivity in wireless sensor networks [1*, 2*, 3*].

2.1 DOA Estimation

Among the parameters that can be estimated as mentioned previously a parameter of particular interest and that has received special attention in the signal processing field is the DOA. The power of knowing the DOAs of signals arriving over an antenna array explains why this parameter is so special. Once one has knowledge of the DOAs of the received signal the received signals may be spatially filtered, effectively separation the signal received from a given direction from the signals received from all the remaining directions. The DOAs are also one of the main parameters of radar systems as the one proposed as a precise radio altimeter in [4*] and are specially important in electronic warfare. Another important upcoming application of DOA estimation is allowing precise navigation of unmanned aerial vehicles (UAVs) as seen in [5*].

The problem of DOA estimation with antenna arrays can be seen in Figure 2.1. The array shown in this figure is known as a uniform linear array (ULA) and has the very interesting properties. For a signal with a given DOA there is a exact and unique phase different between the signals received at adjacent antennas, i.e, there is no ambiguity with respect to DOA. Thus, for this kind

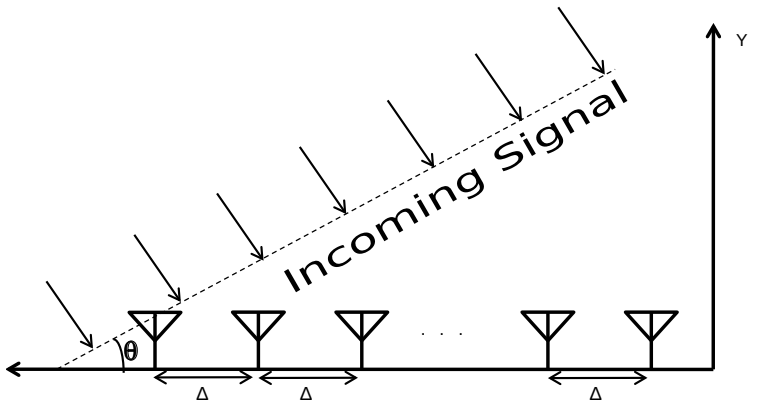

Figure 2.1: Signal arriving at an antenna array and its respective DOA

of arrays, if there is only one signal, one can estimate the DOAs by looking only at this phase difference. Even when more than one signal is present this type of arrays still offers a large number of advantages and is the kind of array assumed in most of the DOA estimation literature.

Although precise DOA estimation is possible in arrays of arbitrary response by employing the very computationally demanding classical maximum likelihood (ML) method [3, 4] or its extensions such as the expectation maximization (EM) [5, 6, 7, 8] or the space alternating generalized expectation maximization (SAGE) [9, 10] these extensions cannot be guaranteed to converge to its local maxima, requiring a good initialization of the parameters, and can be very computationally demanding as the number of wavefronts with parameters to be estimated grow [11]. Another alternative for DOA estimation in arbitrary array geometries is the conventional beamformer [12], this method requires a peak search and cannot properly separate closely spaced wavefronts unless a very large number of antennas is present at the array. An improvement over the conventional beamformer is the CAPON-MVDR [13]. This method offers increased resolution when compared with the traditional beamformer but suffers in the presence of highly correlated wavefronts in very high signal to noise ratio (SNR) scenarios and still requires a peak search. The Multiple SIgnal Classification (MUSIC) [25] algorithm is a subspace based algorithm that can be applied with arrays of arbitrary response, this method also requires a peak search.

As an efficient and precise alternative to DOA estimation a vast number of algorithms that are either close form or require very few iterations have been proposed. Examples of such techniques are the Iterative Quadratic Maximum Likelihood (IQML) [26], Root Weighted Subspace Fitting (Root-WSF) [27] and Root-MUSIC [21] methods. However, all of these methods rely on a Vandermonde or centro-hermitian array response. Another important property a centro-hermitian array response is to allow the application Spatial Smoothing (SPS) [14] and Forward Backward Averaging (FBA) [15]. These techniques enable the application of precise closed form DOA estimation methods and precise model order estimation (estimation of the number of impinging wavefronts) in the presence of highly correlated or even coherent signals. Another important DOA estimation technique is the Estimation of Signal Parameters via Rotational Invariance (ESPRIT) algorithm, this technique requires a shift invariant array response, this is less demanding when compared to a Vandermonde response.

Family	Methods
Maximum Likelihood	Classical ML
	EM
	SAGE
	IQML
Beamformers	Classical beamformer
	CAPON-MVDR
Subspace Methods	MUSIC
	Root-MUSIC
	ESPRIT
	Root-WSF

Table 2.1: Summary of DOA estimation methods

2.2 Array Interpolation

To obtain an array response that is Vandermonde or centro-hermitian is very hard in reality due to effects such as mutual coupling of the antennas, changes in antenna location, material tolerances, hardware biases, and the surrounding environment of the array. Even when the construction is possible there is no guarantee that the response of such an array will be kept invariant over time, e.g. due to wear and temperature stability. A solution to these limitations array interpolation (mapping) was proposed [28] where an arbitrary array response is mapped onto the desired Vandermonde or centro-hermitian response. This mapping is done by obtaining a mapping/transformation matrix **B** capable of transforming the array according to Figure 2.2. Most

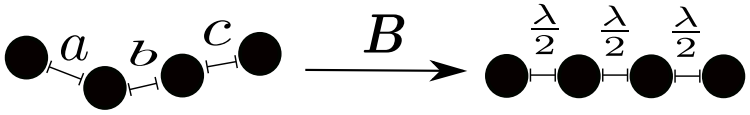

Figure 2.2: Graphical representation of transformation matrix

array interpolation schemes divide the complete angular region into limited angular sectors. For each sector a mapping/transformation matrix is defined using knowledge of the empirical measured array response. Then after transformation to a desired virtual array, FBA or SPS [16] and DOA estimation algorithms such as Root-MUSIC [17] can be applied. However, when performing array interpolation with a sector-by-sector processing the mapping matrices have to be carefully derived in order to minimize the transformation bias within each sector and on the other hand to control its out-of-sector response. The out-of-sector response was neglected in earlier works [16, 17, 18, 19]. Addressing the out-of-sector response by a signal adaptive weighting and a sector-by-sector estimation of highly correlated and closely spaced signal environments is proposed in [23] and [24]. Furthermore, although before the array interpolation the noise is white, after the array interpolation the noise becomes colored. Therefore, a prewhitening step is necessary for MUSIC [20] and Root-MUSIC algorithms [21, 17]. Such prewhitening would destroy the shift invariance properties necessary for the standard ESPRIT algorithm [22]. Array interpolation techniques that

allow the application of a modified ESPRIT algorithm have been proposed in [29] and [30]. These techniques do not require the prewhitening step, thus allowing the direct application of the ESPRIT algorithm. However, they ignore the out-of-sector response and they do not consider the application of FBA or/and SPS and thus cannot be applied with highly correlated signals.

Another application of the array interpolation technique can be seen in [31] where the Vandermonde Invariance Transformation (VIT) was developed. The VIT does not try to address the physical imperfections of the array response but instead transforms the response of an array with a uniform Vandermonde response into one with a non uniform phase response. The VIT provides a noise shaping effect by lowering the noise power over a desired angular region and allowing a more precise DOA estimation at the cost of increased computational load.

The current state of array interpolation divides the field of views of the array into many sectors and requires that an independent DOA estimation is performed for each of these sectors leading to some problems:

- There is no guarantee regarding the behavior of possible out-of-sector signals, possibly introducing bias in the in-sector estimates. Addressing entire field of view leads to large transformation induced bias.
- Deciding the number of signals present at each sector. Can the out-of-sector signals be counted out?
- Choosing between multiple estimates from the different sectors. Do they belong to the same signal or are they estimates of different signals?
- How does the transformation behave when the knowledge of the real array response is corrupted by errors?

2.3 Proposed Array Interpolation Approach

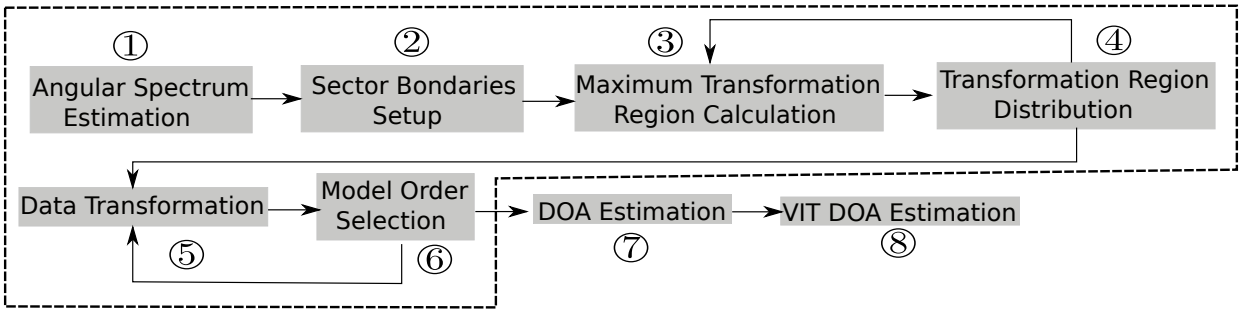

Figure 2.3: Flowchart of proposed approach

The approach proposed in this work is signal adaptive, and tries to address these problems. The proposed approach can be divided into eight different steps as shown in Figure 2.3. The area highlighted by the dashed line relates to the calculation of an optimal transformation that solves the aforementioned problems and is the focus of this work.

In ①, to avoid the classical sector-by-sector processing, a first rough estimate of the regions of the field of view where significant power is arriving is obtained. This estimation is very simple and computationally undemanding.

In ② the results of the first step are used to decided what regions of the field of view are worth transforming and what regions contain only noise can be be left unchanged. This step is also extremely simple and can be done very fast.

In ③ and ④ the results of ② are used to decide how to better apply the transformation over the detected regions, this step aims to ensure that the transformation itself does not introduce large imprecisions in the final DOA estimation while still trying to transform the maximum possible region of the filed of view of the array.

In ⑤ and ⑥ an optimal transformation that takes into account the received noise is set up and the data is transformed while applying the FBA and the SPS for signal decorrelation only when necessary by. This ensures the best possible trade-off between signal decorrelation and loss of array resolution. This step also solves the problem of estimating the number of signals that is present in the classic approaches, since the transformation takes into account all the received signals, the number of signals can be easily estimates using a model order selection method.

In ⑦ we apply the ESPRIT algorithm to estimate the DOA of all incoming signals at once. This step solves many of the problems pointed in the classical array interpolation approaches, since all signals are estimated there is no more out of sector signals and there is no need to choose between different estimates since they are all real estimates.

Finally, in ⑧ the VIT is used to achieve even better DOA estimates. Unfortunately this increased accuracy comes at the cost of increased computational complexity. On the other hand, this step is optional and can be applied if the system has enough idle time or processing power only.

2.4 Applications

The proposed method can be applied to the vast majority of systems that rely on sensor arrays, e.g, radar systems, channel sounding and sonars. As very limited examples of the power of array transformation and of the proposed technique we present two different applications. The first regards the Global Navigation Satellite Systems (GNSS). In these systems the signal is constituted of a line of sight component and highly correlated or even coherent multipath components as well as spoofing. We also consider the application of the proposed technique in sensor mapping in Wireless Sensor Networks (WSNs) where the antenna array is in fact constructed of the various different sensors present in the network.

2.4.1 Antenna Array GNSS Receiver

In the GNSS application the objective is to estimate the time delay of the Line of Sight (LOS) signal. For this purpose a proposed system is presented in Figure 2.4.

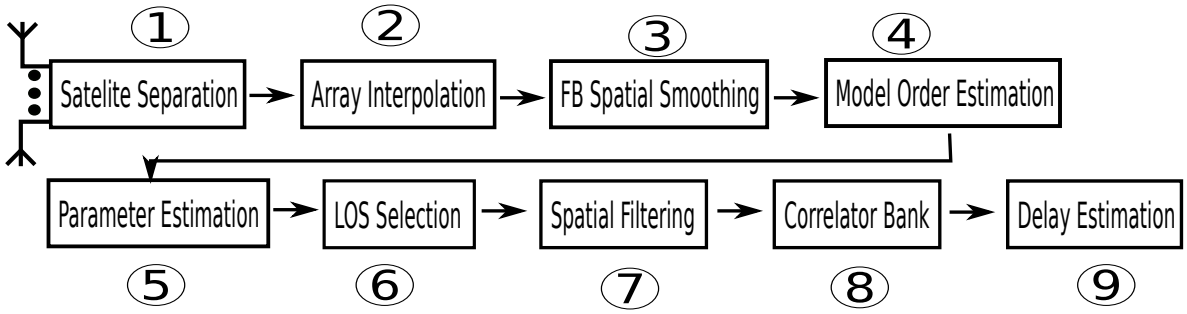

Figure 2.4: Block diagram of the proposed system

In ① the data from the multiple satellites can be separated since GNSS satellites transmit a code division multiple access (CDMA) signal. Separating the signals from the different satellites is extremely important to limit the number of antennas necessary at the array.

In ②, ③, ④ and ⑤ we apply the transformation technique proposed in this work.

In ⑥ we select between all the estimated signals with signal is the line of sight (LOS) component coming from the true satellite. This step eliminates discards possible interferer such as jammers and spoofers, a reality in military environments.

In ⑦, using the estimated DOAs we can filter out all the unwanted signals, leaving only the LOS signal. This is a very important step to allow precise delay estimation.

In ⑧ a correlator bank is proposed to act as an antenna array in time instead of space. This allows the application of known high resolution DOA estimation techniques to estimate the delay of the received and separated LOS satellite signal.

Finally in ⑨ a high resolution DOA estimation method, the MUSIC algorithm, is used to achieve precise delay estimation.

2.4.2 Wireless Sensor Network as an Antenna Array

In the WSN application we propose a simple localization method for sensors in WSNs. The proposed method does not require any external agent, such as a GNSS signal, and requires only a simple crossed dipole antenna. The hardware and software implementations of the proposed method are simple, allowing it to be employed in the extremely hardware limited components of WSNs. The estimated locations of the sensors is used to apply the proposed transformation algorithm effectively turning a WSN with sensors that were randomly place in space, for instance, dropped from an airplane, into a fully functional antenna array with any desired geometry as shown in Figure 2.5. This virtual antenna array can be used, for instance, to get rid of any interfering signal that comes from outside of the sensor network.

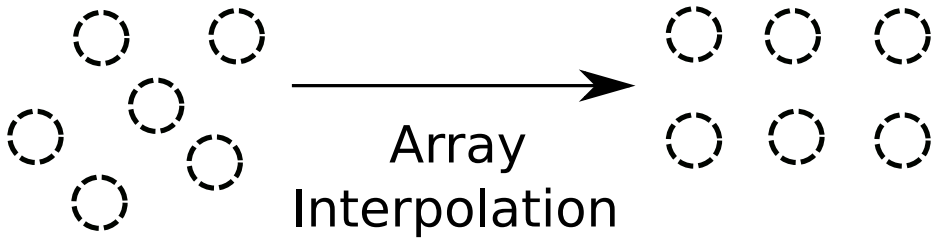

Figure 2.5: Example of WSN transformed into virtual antenna array

The remainder of this thesis is divided as follows. The signal model used in this thesis is detailed in Chapter 3. The theoretical and mathematical foundation of the steps proposed for the transformation are explained in detail in Chapter 4. The two applications are detailed in Chapter 5. Finally, in Chapter 6 conclusions are drawn.

2.5 Contributions

This work presents a novel array interpolation method capable of achieving improved precision in DOA estimation when compared to the current state-of-the-art array interpolation techniques present in the literature. The proposed method deals with problems that were previously present, as the presence of "ghost" signals, signals that are estimated even thought they are not actually present in the array. It also consider problems that were left unmentioned in previous works, such as the estimation of the number of signals received on the array after interpolation has be applied.

The proposed approach is used to build an improved GNSS receiver capable of dealing with heavily correlated signals that would normally result in decreased performance in normal GNSS receivers. The proposed approach is also used to transform a WSN into a fully functional antenna array, thus transforming the WSN into a robust a versatile system.

Chapter 3

Data Model

3.1 Notation

Throughout this work matrix will be denoted with uppercase upright bold letters $\mathbf{X}$, vectors will be denoted with lower case upright bold letters $\mathbf{x}$, variables will be denoted with lowercase italic letters k, the value of the element at the index k of a vector $\mathbf{x}$ will be denoted by $\mathbf{x}[k]$, sets will be denoted with calligraphic letters $\mathcal{S}$.

3.2 Data Model

In this chapter we present the data model for the GNSS, this is the most complete and complex data model used in this work. However, part of the data model and its respective notation may not be always necessary and will be dropped on some sections for clarity and simplicity.

We assume L narrow band waves are received by a system composed of a array doublets of antennas polarized with Right Hand Circular Polarization (RHCP) and Left Hand Circular Polarization (LHCP). The distance between the transmitter antenna and receiver array is considered long enough so that all impinging wave forms can be treated as planar. The distance between the antennas elements in the array is not assume to be invariant, as shown in Figure 3.1.

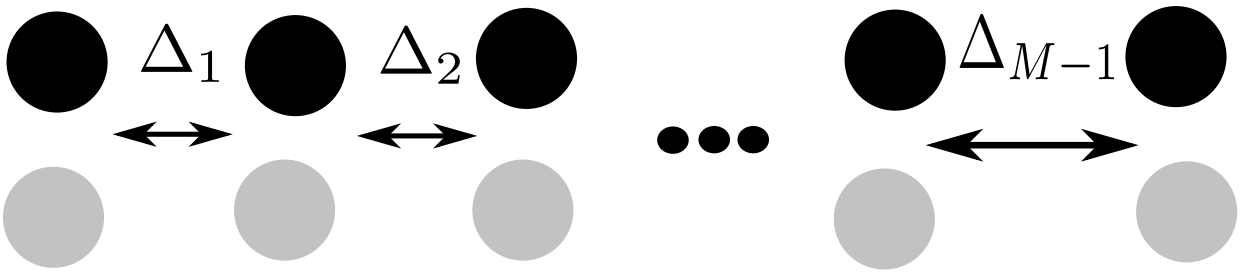

Figure 3.1: Linear array consisting of pairs of diversely polarized antennas.

The signals transmitted by the GPS satellite systems are RHCP, this polarization is chosen

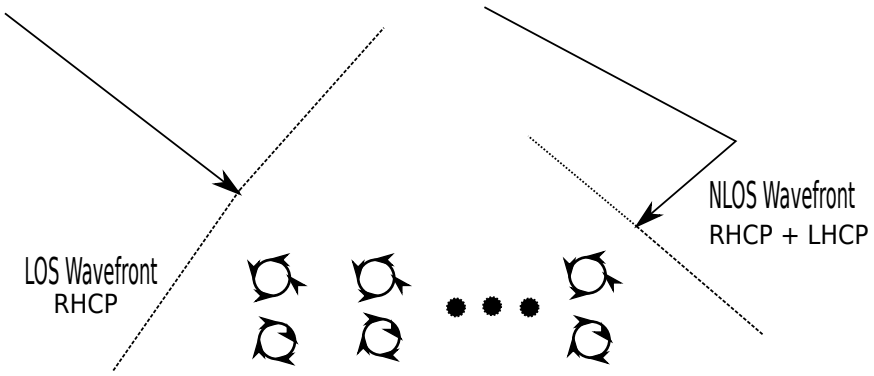

Figure 3.2: Example of wavefronts impinging over the dual polarized array

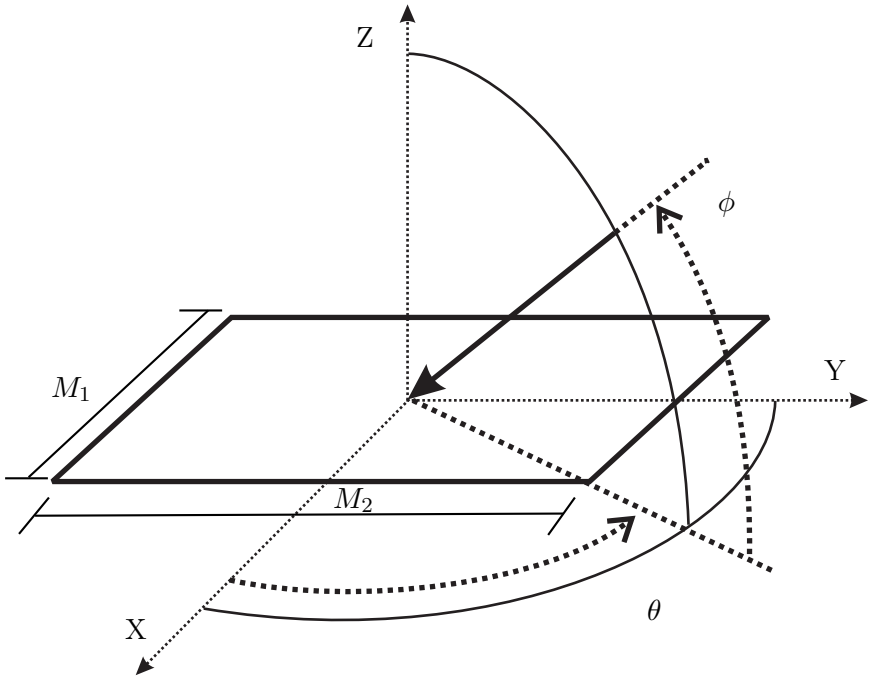

Figure 3.3: Graphical representation of a $M_1 \times M_2$ array

so that the received signal does not depend on the position of the receiver antenna and also to mitigate some effects caused by the transmission trough the Ionosphere. When a RHCP signal is reflected its polarization is affected, resulting in a signal that will usually be present at both antenna outputs. This work tries to take advantage of the extra information available when dealing with dual polarized antennas. Figure 3.2 illustrates this effect over the dual polarized array.

Considering an antenna array composed of $M_1 \times M_2$ dual polarization doublets as displayed on Figure 3.3

the received signal at time instant t can be expressed as

$$x(t) = \mathbf{s}(t) + \mathbf{z}(t) + \mathbf{n}(t) = \sum_{\ell=1}^{d} \mathbf{s}_\ell(t) + \sum_{\imath=1}^{I} \mathbf{z}_\imath(t) + \mathbf{n}(t), \tag{3.1}$$

where $\mathbf{s}(t) \in \mathbb{C}^{2 \cdot M_1 \cdot M_2 \times 1}$ denotes the superimposed signal replicas

$$\mathbf{s}_\ell(t) = [\mathbf{a}(\phi_\ell, \vartheta_\ell) \otimes \mathbf{u}(\phi_\ell, \vartheta_\ell)] \gamma_\ell \mathrm{e}^{\mathrm{j}2\pi\nu_\ell t} c(t - \tau_\ell), \tag{3.2}$$

where $\otimes$ denotes the Kronecker product, $\mathbf{a}(\phi_\ell, \vartheta_\ell) \in \mathbb{C}^{M_1 \cdot M_2 \times 1}$ defines the array steering vector for the ℓ-th signal arriving with azimuth angle ϕ_ℓ and elevation angle ϑ_ℓ. By defining a reference sensor placed at coordinates $(0, 0)$ in the plane formed by the rectangular array, $\mathbf{a}(\phi_\ell, \vartheta_\ell)$ can be constructed as

$$\mathbf{a}(\phi_\ell, \vartheta_\ell) = \begin{bmatrix} \mathrm{e}^{\frac{\mathrm{j}2\pi}{\lambda}\left(\sqrt{x_{1,1}^2+y_{1,1}^2}\cos(\phi_\ell)\sin(\vartheta_\ell)+\sqrt{x_{1,1}^2+y_{1,1}^2}\sin(\phi_\ell)\sin(\vartheta_\ell)\right)} \\ \vdots \\ \mathrm{e}^{\frac{\mathrm{j}2\pi}{\lambda}\left(\sqrt{x_{1,M_2}^2+y_{1,M_2}^2}\cos(\phi_\ell)\sin(\vartheta_\ell)+\sqrt{x_{1,M_2}^2+y_{1,M_2}^2}\sin(\phi_\ell)\sin(\vartheta_\ell)\right)} \\ \mathrm{e}^{\frac{\mathrm{j}2\pi}{\lambda}\left(\sqrt{x_{2,1}^2+y_{2,1}^2}\cos(\phi_\ell)\sin(\vartheta_\ell)+\sqrt{x_{2,1}^2+y_{2,1}^2}\sin(\phi_\ell)\sin(\vartheta_\ell)\right)} \\ \vdots \\ \mathrm{e}^{\frac{\mathrm{j}2\pi}{\lambda}\left(\sqrt{x_{M_1,M_2}^2+y_{M_1,M_2}^2}\cos(\phi_\ell)\sin(\vartheta_\ell)+\sqrt{x_{M_1,M_2}^2+y_{M_1,M_2}^2}\sin(\phi_\ell)\sin(\vartheta_\ell)\right)} \end{bmatrix} \tag{3.3}$$

where $x_{i,j}$ and $y_{i,j}$ denote the coordinates over the x and y axes of the sensor indexed by i, j. $\mathbf{u}(\phi_\ell, \vartheta_\ell) \in \mathbb{C}^{2\times 1}$ defines the vector of the form

$$\mathbf{u}(\phi_\ell, \vartheta_\ell) = [u_{\mathrm{R}}(\phi_\ell, \vartheta_\ell), u_L(\phi_\ell, \vartheta_\ell)]^{\mathrm{T}} \tag{3.4}$$

where $u_{\mathrm{R}}(\phi_\ell, \vartheta_\ell)$ and $u_L(\phi_\ell, \vartheta_\ell)$ are complex elements related to the gains and the "bleed trough" caused by antenna coupling or circuit imperfection of the diversely polarized sensors as shown in Figure 3.4 and, for the sake of completeness, are assumed to depend on the angles of arrival of the impinging waves since perfect uni-directionality cannot be guaranteed. From here on these elements shall be refereed to as antenna factors. γ_ℓ is the complex amplitude, ν_ℓ is the Doppler frequency, $c(t - \tau_\ell)$ denotes a periodically repeated pseudo random (PR) sequence $c(t)$ with time delay τ_ℓ, chip duration T_c and period $T = N_c T_c$, with $N_c \in \mathbb{N}$, and $\mathbf{z}(t) \in \mathbb{C}^{2 \cdot M_1 \cdot M_2 \times 1}$ denotes superimposed radio interference signals where

$$\mathbf{z}_\imath(t) = [\mathbf{a}(\phi_\imath, \vartheta_\imath) \otimes \mathbf{u}(\phi_\imath, \vartheta_\imath)] b_\imath(t), \tag{3.5}$$

and $b_\imath(t)$ defines the $\imath$-th radio interference signal with $\imath = 1, ..., I$. $\mathbf{n}(t) \in \mathbb{C}^{2 \cdot M_1 \cdot M_2 \times 1}$ denotes the noise present at times instant t, no assumption is made regarding the structure of the noise, i.e, the noise is not assumed to be either spatially or temporally uncorrelated. In the following the parameters of the LOS signal are indicated with $\ell = 1$ and the parameters of the NLOS signals (multi-path) with $\ell = 2, ..., L$.

The spatial observations are collected at K periods of the PR sequence at N time instances, thus $\mathbf{x}[(k-1)N + n] = \mathbf{x}[((k-1)N + n)T_s]$ with $n = 1, ..., N$, $k = 1, ..., K$, $\frac{1}{T_s} \geq 2B$. The channel parameters are assumed constant during the k-th period of the observation interval. Collecting the samples of the k-th period of the observation interval we define the $2 \cdot M_1 \cdot M_2 \times N$ complex

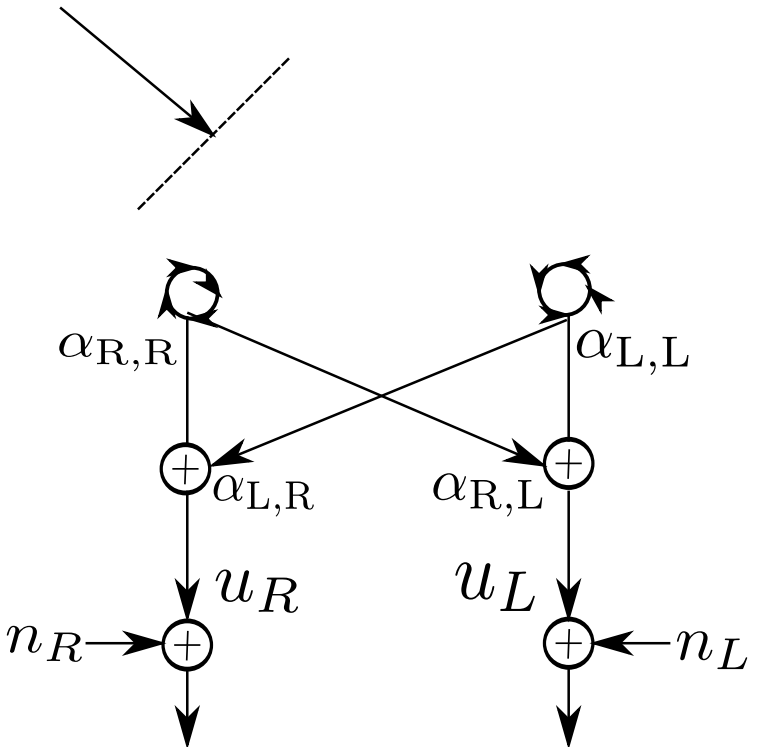

Figure 3.4: Detailed diagram of a diversely polarized pair.

matrices:

$$\mathbf{X}[k] = [\mathbf{x}[(k-1)N+1], ..., \mathbf{x}[(k-1)N+n], ..., \mathbf{x}[(k-1)N+N]], \tag{3.6}$$

$$\mathbf{N}[k] = [\mathbf{n}[(k-1)N+1], ..., \mathbf{n}[(k-1)N+n], ..., \mathbf{n}[(k-1)N+N]], \tag{3.7}$$

$$\mathbf{S}[k] = [\mathbf{s}[(k-1)N+1], ..., \mathbf{s}[(k-1)N+n], ..., \mathbf{s}[(k-1)N+N]], \tag{3.8}$$

$$\mathbf{Z}[k] = [\mathbf{z}[(k-1)N+1], ..., \mathbf{z}[(k-1)N+n], ..., z[(k-1)N+N]]. \tag{3.9}$$

Thus, the signal can be expressed in matrix notation as

$$\begin{aligned} \mathbf{X}[k] &= \mathbf{S}[k] + \mathbf{Z}[k] + \mathbf{N}[k] \\ &= (\mathbf{A}_s[k] \diamond \mathbf{U}_s[k])\mathbf{\Gamma}[k](\mathbf{C}[k] \odot \mathbf{D}[k]) \\ &+ (\mathbf{A}_z[k] \diamond \mathbf{U}_z[k])\mathbf{G}[k] + \mathbf{N}[k], \end{aligned} \tag{3.10}$$

where $\odot$ denotes the Hadamard-Schur product, $\diamond$ denotes the Khatri-Rao product,

$$\mathbf{A}_s[k] = [\mathbf{a}(\phi_1, \vartheta_1), ..., \mathbf{a}(\phi_\ell, \vartheta_\ell), ..., \mathbf{a}(\phi_L, \vartheta_L)] \in \mathbb{C}^{M_1 \cdot M_2 \times L} \tag{3.11}$$

and

$$\mathbf{A}_z[k] = [\mathbf{a}(\phi_1, \vartheta_1), ..., \mathbf{a}(\phi_\imath, \vartheta_\imath), ..., \mathbf{a}(\phi_I, \vartheta_I)] \in \mathbb{C}^{M_1 \cdot M_2 \times I} \tag{3.12}$$

denote the steering matrices,

$$\mathbf{U}_s[k] = [\mathbf{u}(\phi_1, \vartheta_1), ..., \mathbf{u}(\phi_\ell, \vartheta_\ell), , ..., \mathbf{u}(\phi_L, \vartheta_L)] \in \mathbb{C}^{2 \times L} \tag{3.13}$$

and

$$\mathbf{U}_z[k] = [\mathbf{u}(\phi_1, \vartheta_1), ..., \mathbf{u}(\phi_\imath, \vartheta_\imath), , ..., \mathbf{u}(\phi_I, \vartheta_I)] \in \mathbb{C}^{2 \times I} \tag{3.14}$$

are the matrices containing the antenna factors,

$$\mathbf{\Gamma}[k] = \mathrm{diag}\{\gamma\} \in \mathbb{C}^{L\times L} \tag{3.15}$$

is a diagonal matrix whose entries are complex amplitudes of the signal replicas $\gamma = [\gamma_1, ..., \gamma_\ell, ..., \gamma_L]^{\mathrm{T}}$,

$$\mathbf{C}[k] = [\mathbf{c}[k,\tau_1]...\mathbf{c}[k,\tau_\ell]...\mathbf{c}[k,\tau_L]]^{\mathrm{T}} \in \mathbb{C}^{L\times N} \tag{3.16}$$

contains the sampled and shifted $c(t)$ for each impinging wavefront

$$\begin{aligned}\mathbf{c}[k,\tau_\ell] &= [c(((k-1)N+1)T_s-\tau_\ell), ..., c(((k-1)N+n)T_s-\tau_\ell),\\ &\quad ..., c(((k-1)N+N)T_s-\tau_\ell)]^{\mathrm{T}}\end{aligned} \tag{3.17}$$

$$\mathbf{D}[k] = [\mathbf{d}[k,\nu_1]...\mathbf{d}[k,\nu_\ell]...\mathbf{d}[k,\nu_L]] \in \mathbb{C}^{L\times N} \tag{3.18}$$

contains the complex exponential functions conveying the Doppler frequency of each wavefront

$$\begin{aligned}\mathbf{d}[k,\nu_\ell] &= [\mathrm{e}^{\mathrm{j}2\pi\nu_\ell((k-1)N+1)T_s}, ..., \mathrm{e}^{\mathrm{j}2\pi\nu_\ell((k-1)N+n)T_s},\\ &\quad \mathrm{e}^{\mathrm{j}2\pi\nu_\ell((k-1)N+N)T_s}]^{\mathrm{T}}\end{aligned} \tag{3.19}$$

and

$$\mathbf{G}[k] = [\mathbf{g}_1[k]...\mathbf{g}_\imath[k]...\mathbf{g}_I[k]] \in \mathbb{C}^{I\times N} \tag{3.20}$$

contains the sampled $b_\imath(t)$ of each interference waveform

$$\begin{aligned}\mathbf{g}_\imath[k] &= [[g_\imath(((k-1)N+1)T_s), ..., g_\imath(((k-1)N+n)T_s,\\ &\quad g_\imath(((k-1)N+N)T_s]^{\mathrm{T}}.\end{aligned} \tag{3.21}$$

Note that the resulting $\mathbf{X}$ matrix for a given period k contains the measurements of one snapshot stacked along one column, with the snapshots taken along different dimensions stacked along its rows. This results in a matrix of the type

$$\mathbf{X} = \begin{bmatrix} x_{1,1,1,1} & x_{1,1,1,2} & \cdots & x_{1,1,1,N}\\ x_{1,1,2,1} & x_{1,1,2,2} & \cdots & x_{1,1,2,N}\\ x_{1,2,1,1} & x_{1,2,1,2} & \vdots & x_{1,2,1,N}\\ \vdots & \vdots & \cdots & \vdots\\ x_{1,M_2,2,1} & x_{1,M_2,2,2} & \cdots & x_{1,M_2,2,N}\\ x_{2,1,1,1} & x_{2,1,1,2} & \cdots & x_{2,1,1,N}\\ \vdots & \vdots & \vdots & \vdots\\ x_{M_1,M_2,2,1} & x_{M_1,M_2,2,2} & \cdots & x_{M_1,M_2,2,N}\end{bmatrix} \in \mathbb{C}^{2M_1M_2\times N}, \tag{3.22}$$

where the third index corresponds to the polarization of the respective measurement with 1 being the RHCP and 2 being the LHCP measurements.

The received signal covariance matrix $\mathbf{R}_{\mathbf{XX}} \in \mathbb{C}^{M\times M}$ is given by

$$\mathbf{R}_{\mathbf{XX}} = \mathrm{E}\{\mathbf{X}\mathbf{X}^{\mathrm{H}}\} = (\mathbf{A}_s[k]\diamond\mathbf{U}_s[k])\mathbf{R}_{\mathbf{SS}}(\mathbf{A}_s[k]\diamond\mathbf{U}_s[k])^{\mathrm{H}} \tag{3.23}$$

$$+ (\mathbf{A}_z[k]\diamond\mathbf{U}_z[k])\mathbf{R}_{\mathbf{GG}}(\mathbf{A}_z[k]\diamond\mathbf{U}_z[k])^{\mathrm{H}} + \mathbf{R}_{\mathbf{NN}}, \tag{3.24}$$

where $(\centerdot)^{\mathrm{H}}$ stands for the conjugate transposition, and

$$\mathbf{R_{SS}} = \begin{bmatrix} \sigma_1^2 & \rho_{1,2}\sigma_1\sigma_2 & \cdots & \rho_{1,d}\sigma_1\sigma_d \\ \rho_{1,2}^*\sigma_1\sigma_2 & \sigma_2^2 & & \vdots \\ \vdots & & \ddots & \\ \rho_{1,d}^*\sigma_1\sigma_d & \rho_{2,d}^*\sigma_2\sigma_d & \cdots & \sigma_d^2 \end{bmatrix}, \tag{3.25}$$

where σ_i^2 is the power of the $i-$th signal and $\rho_{a,b} \in \mathbb{C}$, $|\rho_{a,b}| \leq 1$ is the cross correlation coefficient between signals a and b. $\mathbf{R_{NN}} \in \mathbb{C}^{M \times M}$ the noise covariance matrix.

The estimate of the signal covariance matrix can be found by

$$\hat{\mathbf{R}}_{\mathbf{XX}} = \frac{\mathbf{X}\mathbf{X}^{\mathrm{H}}}{N}. \tag{3.26}$$

Chapter 4

Signal Adaptive Iterative Reduced Rank Array Interpolation

Parameter estimation methods for narrow band signals have received significant attention over the course of the last three decades. The subspace based methods present very interesting properties, being very robust to noise and capable of high precision even when the signal power is bellow the noise floor. Another very important property of such methods is that their computational complexity can be made very low, for instance, with the ESPRIT algorithm, when compared to maximum likelihood methods while not sacrificing so much precision [32].

These methods, however, rely on a full rank signal covariance matrix, that is, they require that the received signals are not highly correlated. While this may be true for some systems, its high unlikely that a very similar signal would be transmitted from two different directions, that is not always the case. Close multipath components of the same signal or unfriendly jamming signals will present a very high correlation coefficient, leading to a rank-deficient signal covariance matrix and resulting in signal eigenvectors showing up on the noise subspace and producing largely imprecise estimates specially for closely spaced signals [33]. To apply subspace based methods in highly correlated signal environments the application of signal decorrelating methods is necessary, for such end the Spatial Smoothing (SPS) [14] and Forward Backward Averaging (FBA) [15] can be used.

Applying SPS or FBA demands an array with a very specific response, a Vandermonde response. A simple geometry capable of attaining a Vandermonde response is the uniform array, in such arrays the antennas elements are separated by a precise and invariant distance, furthermore it is necessary that for a given direction of arrival all the antenna elements introduce the same amplitude and phase attenuation on the received signal, i.e, perfect calibration. Constructing antenna arrays with such precision is not aways possible and even when possible it is not possible to achieve perfect calibration due to effects such as mutual coupling of antennas. To allow the application of SPS and FBA in antenna arrays of arbitrary geometry and with imperfect responses array interpolation methods are used.

In this chapter we detail the Spatial Smoothing and Forward Backward Averaging we also

present a overview of classical array interpolation methods present in the literature and their limitations. A new array interpolation method is presented and its results are compared to the current state-of-the-art method available for using array interpolation to deal with highly correlated signals.

4.1 Forward Backward Averaging

In the case where only two highly correlated or coherent sources are present the Forward Backward Averaging [15] is capable of decorrelating the signals and allowing the application of subspace base methods. For an uniform linear array (ULA) or uniform rectangular array (URA) the steering vectors remain invariant, up to scaling, if their elements are reversed and complex conjugated. Let $\mathbf{Q} \in \mathbb{Z}^{M\times M}$ by an exchange matrix with ones on its anti-diagonal and zeros elsewhere such as

$$\mathbf{Q} = \begin{bmatrix} 0 & 0 & 0 & 1 \\ 0 & 0 & 1 & 0 \\ 0 & 1 & 0 & 0 \\ 1 & 0 & 0 & 0 \end{bmatrix}, \tag{4.1}$$

then, for a M element ULA it holds that

$$\mathbf{Q}\mathbf{A}^{*} = \mathbf{A}. \tag{4.2}$$

The FBA covariance matrix can be obtained as

$$\hat{\mathbf{R}}_{\mathbf{XX}_{FBA}} = \frac{1}{2}(\hat{\mathbf{R}}_{\mathbf{XX}} + \mathbf{Q}\hat{\mathbf{R}}^{*}_{\mathbf{XX}}\mathbf{Q}). \tag{4.3}$$

By looking into the structure of the covariance matrix shown in (3.23), (4.3) can be rewritten as

$$\hat{\mathbf{R}}_{\mathbf{XX}_{FBA}} = \mathbf{A}\frac{1}{2}(\mathbf{R}_{\mathbf{SS}} + \mathbf{R}^{*}_{\mathbf{SS}})\mathbf{A}^{\mathrm{H}} + \frac{1}{2}(\mathbf{R}_{\mathbf{NN}} + \mathbf{Q}\mathbf{R}_{\mathbf{NN}}{}^{*}\mathbf{Q}). \tag{4.4}$$

The results is that the matrix $\mathbf{R}_{\mathbf{SS}} + \mathbf{R}^{*}_{\mathbf{SS}}$ is composed of purely real numbers, that is, if the correlation coefficient between the signals is given by a purely imaginary number then the FBA offers maximum decorrelation, if, however, the correlation coefficient is given only by a real number, then the FBA offers no improvement regarding signal decorrelation. FBA can also be used with the sole purpose of improving the variance of the estimates.

4.2 Spatial Smoothing

In scenarios where more than two highly correlated sources are present the FBA alone cannot restore the full rank of the signal covariance matrix by itself and thus another solution is necessary. Spatial Smoothing was first presented as a heuristic solution in [34] and extended to signal processing in [14]. The idea behind Spatial Smoothing is to split a uniform array into multiple overlapping subarrays as shown in Figure 4.1, the steering vectors of the subarrays are again assumed to be identical up to scaling, therefore the covariance matrices of each subarray can be averaged.

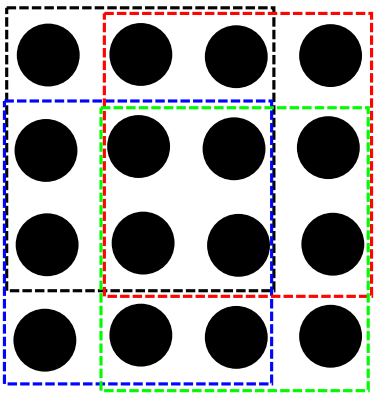

Figure 4.1: Example of SPS subarrays

Spatial Smoothing induces a random phase modulation that tends to decorrelate the signals that cause the rank deficiency [32]. The SPS covariance matrix can be written as

$$\hat{\mathbf{R}}_{\mathbf{XX}_{SPS}} = \frac{1}{V}\sum_{v=1}^{V} \mathbf{J}_v \hat{\mathbf{R}}_{\mathbf{XX}} \mathbf{J}_v^{\mathrm{T}}, \tag{4.5}$$

where $\mathbf{J}_v$ is an appropriate selection matrix.

The rank of the SPS covariance matrix can be shown to increase by 1 with probability 1 [35] for each additional subarray used until it reaches the maximum rank of L. Spatial Smoothing however comes at the cost of reducing array aperture, since the subarrays are composed of less antennas than the original full array.

4.3 Model Order Selection

Model order selection is selecting the optimal trade-off between model resolution and its statistical reliability. In the specific case of this work, model order selection is mostly employed to select the eigenvectors of the signal covariance matrix that account for most of its power, each of these eigenvectors in turn represent the statistics of a received signal. Therefore, in this work, model order selection is mostly used to estimate the number of signals received at the antenna array. This is done by analyzing the profile of the eigenvalues of the signal covariance matrix and looking for a big gap that should separate the eigenvalues related to the signal from the ones related to the noise. If the signals are highly correlated a single eigenvalue can be related to two or more signals, with in turn will lead to a biased estimation. For this reason the aforementioned FBA and SPS must be applied in such cases.

Figure 4.2 presents the example of an eigenvalue profile of two incoming signals after Forward Backward Averaging and Spatial Smoothing have been applied. The SNR is this case is 30 dB and eight antennas are used. Note that visually identifying the model order is very difficult. To address this problem techniques that were originally developed for model fitting is statistical models were extended to detecting the number of signals impinging over an antenna array. Model order selection schemes such as the AIC and the MDL methods [36] and more recently the RADOI [37] are capable

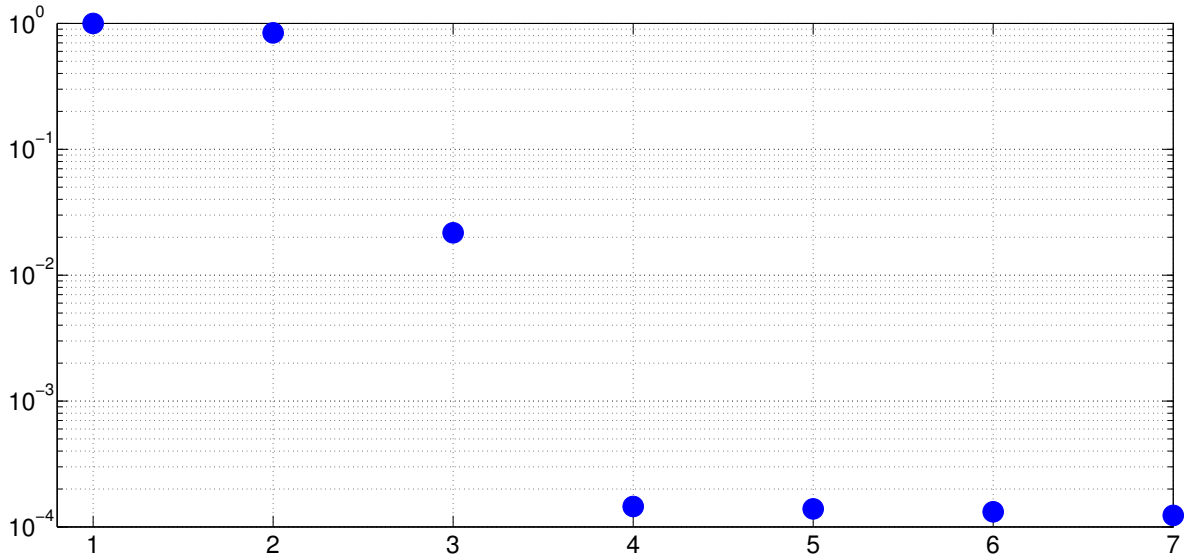

Figure 4.2: Eigenvalue profile: eigenvalue index versus eingenvalue

of properly detection the number of signals incoming in the eigenvalue profile shown in Figure 4.2. For multidimensional problems more accurate methods such as [38], [39] can be used.

4.4 Classical Array Interpolation

The SPS and FBA methods shown for decorrelating signals are limited to arrays of uniform geometry. As mentioned previously such geometries are hard to achieve in real implementations due to problems such as space limitation or the non linearity of the antenna lobes with respect to the direction of arrival of received waves. Also, important subspace DOA estimation methods such as the Root-MUSIC [21] rely on the ULA geometry and although the ESPRIT [22] requires only the shift invariance property, in the literature most authors apply ESPRIT in either a ULA or URA. Thus, to allow the application of such methods is generic arrays some sort of data transformation needs to be used first. This type of transformation of known in the literature are array interpolation or array mapping. The basic idea behind array interpolation is trying to predict what would be the data received at an array with a desired specific geometry based on the data received on a real arbitrarily array.

Array interpolation seeks to find a transformation matrix $\mathbf{B}$ that satisfies

$$\mathbf{BA} = \bar{\mathbf{A}}, \tag{4.6}$$

where $\mathbf{A}$ and $\bar{\mathbf{A}}$ are the real and desired array steering matrices respectively. In classical array interpolation, since the receiver has no prior information about the DOA of the received signals $\mathbf{A}$ and $\bar{\mathbf{A}}$ are constructed by dividing the field of view of the array into W continuous regions, called sectors, with upper bound u_w and lower bound l_w. The region $[l_w, u_w]$ is then discretized according to

$$\mathcal{S}_w = [l_w, l_w + \Delta, ..., u_w - \Delta, u_w], \tag{4.7}$$

where Δ is the angular resolution of the transformation. These angles are used to generate the respective set of steering vectors and construct $\mathbf{A}$ and $\bar{\mathbf{A}}$ according to

$$\mathbf{A}_{\mathcal{S}_w} = [\mathbf{a}(l_w), \mathbf{a}(l_w + \Delta), ..., \mathbf{a}(u_w - \Delta), \mathbf{a}(u_w)] \in \mathbb{C}^{M \times \frac{u_w - l_w}{\Delta}},$$

$$\bar{\mathbf{A}}_{\mathcal{S}_w} = [\bar{\mathbf{a}}(l_w), \bar{\mathbf{a}}(l_w + \Delta), ..., \bar{\mathbf{a}}(u_w - \Delta), \bar{\mathbf{a}}(u_w)] \in \mathbb{C}^{M \times \frac{u_w - l_w}{\Delta}},$$

where M is the total number of antennas, including their different polarizations, present at the array. The transformation is not usually not perfect since the transformation matrix $\mathbf{B}$ does not have enough degrees of freedom to transform the entire discrete sector. $\mathbf{B}$ is obtained as the best feet between the transformed response $\mathbf{B}\mathbf{A}_{\mathcal{S}_w}$ and the desired response $\bar{\mathbf{A}}_{\mathcal{S}_w}$, this is done by applying a least squares fit to the overdetermined systems yielding

$$\mathbf{B} = \bar{\mathbf{A}}_{\mathcal{S}_w} \mathbf{A}^{\dagger}_{\mathcal{S}_w} \in \mathbb{C}^{M \times M}, \tag{4.8}$$

where $(\cdot)^{\dagger}$ is the pseudo inverse of the matrix. To access the precision of the transformation the Frobenius norm of the errors matrix $\mathbf{B}\mathbf{A}_{\mathcal{S}_w} - \bar{\mathbf{A}}_{\mathcal{S}_w}$ is compared with the Frobenius norm of the desired response steering matrix $\bar{\mathbf{A}}_{\mathcal{S}_w}$. The error of the transform is defined as

$$\epsilon(\mathcal{S}_w) = \frac{\left\| \bar{\mathbf{A}}_{\mathcal{S}_w} - \mathbf{B}\mathbf{A}_{\mathcal{S}_w} \right\|_{\mathrm{F}}}{\left\| \bar{\mathbf{A}}_{\mathcal{S}_w} \right\|_{\mathrm{F}}} \in \mathbb{R}^{+}. \tag{4.9}$$

Large transformation errors will results in a large bias in the final DOA estimates. The transformation error can, however, be kept as low as desired by making the sectors $\mathcal{S}$ smaller. It is worth noting that for this approach of transformation matrix calculation the transformation matrices can be calculated off-line, since they do not rely on the received data, and just reused when necessary.

With $\mathbf{B}$ at hand the data can be transformed by

$$\bar{\mathbf{X}} = \mathbf{B}\mathbf{X}. \tag{4.10}$$

The transformed covariance is then equivalent to

$$\bar{\mathbf{R}}_{\mathbf{XX}} = \frac{\mathbf{B}\mathbf{X}(\mathbf{B}\mathbf{X})^{\mathrm{H}}}{N} = \frac{\mathbf{B}\mathbf{X}\mathbf{X}^{\mathrm{H}}\mathbf{B}^{\mathrm{H}}}{N} = \mathbf{B}\hat{\mathbf{R}}_{\mathbf{XX}}\mathbf{B}^{\mathrm{H}}. \tag{4.11}$$

From (4.11) it is easy to see that the transformation matrix can instead be applied directly to the covariance matrix. By plugging (3.25) into (4.11) we have

$$\begin{aligned} \bar{\mathbf{R}}_{\mathbf{XX}} &= \mathbf{B}\mathbf{A}\mathbf{R}_{\mathbf{SS}}\mathbf{A}^{\mathrm{H}}\mathbf{B}^{\mathrm{H}} + \mathbf{B}\mathbf{R}_{\mathbf{NN}}\mathbf{B}^{\mathrm{H}} \\ &= \bar{\mathbf{A}}\mathbf{R}_{\mathbf{SS}}\bar{\mathbf{A}}^{\mathrm{H}} + \mathbf{B}\mathbf{R}_{\mathbf{NN}}\mathbf{B}^{\mathrm{H}}. \end{aligned} \tag{4.12}$$

Thus, although the transformation transforms $\mathbf{A}$ into $\bar{\mathbf{A}}$ as desired it changes the characteristics of $\mathbf{R}_{\mathbf{NN}}$. If the noise was previously white it becomes colored or, if the noise was already colored, it changes its color. Since most of the methods in the literature assume that $\mathbf{R}_{\mathbf{NN}} = \sigma_n^2\mathbf{I}$, i.e, white noise, the next step used in classical interpolation is a noise whitening step to restore the diagonal characteristic of $\mathbf{R}_{\mathbf{NN}}$

$$\bar{\mathbf{R}}_{\mathbf{XX}} = \bar{\mathbf{R}}_{\mathbf{NN}}^{-\frac{1}{2}} \bar{\mathbf{R}}_{\mathbf{XX}} \bar{\mathbf{R}}_{\mathbf{NN}}^{-\frac{\mathrm{H}}{2}}, \tag{4.13}$$

where $\bar{\mathbf{R}}_{\mathbf{NN}} = \mathbf{B}\mathbf{R}_{\mathbf{NN}}\mathbf{B}^{\mathrm{H}}$. This operation, however, tends to increase bias due to the possible ill conditioning of the original noise covariance and, although it diagonalizes o the noise covariance term again, it affects the signal covariance, and disallows the direct application of ESPRIT, since it destroys the shift invariance, and requires the MUSIC algorithm to be weighted by the term $\bar{\mathbf{R}}_{\mathbf{NN}}^{-\frac{1}{2}}$ used in the prewhitening. Different methods for array interpolation have been specially developed in order to apply the ESPRIT algorithm [30, 29]. In these methods a different transformation matrix is calculated for each of the shift invariant subarrays used in ESPRIT, in this way the noise between each subarray is not correlated and ESPRIT can be directly used, these methods, however, do not allow the application of FBA-SPS and thus are incapable of being used in the presence of highly correlated signals.

All the current approaches in the literature use this sector-by-sector processing, the works in [17], [18] and [19] differ only by the way the matrix $\bar{\mathbf{A}}$ is set up.

The current state-of-the-art for applying array interpolation in highly correlated signals is presented in [23, 24]. Normally, if the signals that fall out-of-sector are not correlated with the in sector signals the influence of the out-of-sector signals in the processing posterior to the transformation is not high. On the other hand, if a signal located out-of-sector is correlated with an in sector signal, the posterior estimations can be gravely affected. These works try to keep the out-of-sector response under control by taking into account the response over the entire array manifold. The problem can be formulated as a weighted least squares problem

$$\min_{\mathbf{T}} \int_{-\pi}^{\pi}\int_{-\pi}^{\pi} w(\phi,\vartheta)\left\|\mathbf{T}\mathbf{a}(\phi,\vartheta) - v(\phi,\vartheta)\bar{\mathbf{a}}(\phi,\vartheta)\right\|^2 \mathrm{d}\phi\,\mathrm{d}\vartheta, \tag{4.14}$$

were $W(\phi,\vartheta)$ is an arbitrary weighting function and $v(\phi,\vartheta)$ defines the DOA dependent gain that shapes the array response, it should control the response of the array for out-of-sector signals while leaving the response unaltered for signals within the sector. An optimal solution would be to set $v(\phi,\vartheta)$ as a rectangular function, setting its gain to zero to any DOA outside of the sector and to 1 for the entire sector. This, however, would result in extremely large transformation errors, specially due to the discontinuities found in the edges of the sector. Another alternative is to shape $v(\phi,\vartheta)$ as a root raised cosine function in ϕ and ϑ, allowing the gain to roll off along the edges of the sector. By defining the sectors $\Delta\phi = [-\phi_0, \phi_0]$ and $\Delta\vartheta = [-\vartheta_0, \vartheta_0]$ the gain is described as

$$v(\phi,\vartheta) = \begin{cases} 1, & |\phi| \leq \phi_0 \text{ and } |\vartheta| \leq \vartheta_0 \\ \frac{1}{2} + \frac{1}{4}\cos(\frac{\pi(|\phi|-\phi_0)}{2\phi_0-\pi}) + \frac{1}{4}\cos(\frac{\pi(|\vartheta|-\vartheta_0)}{2\vartheta_0-\pi}), & \phi_0 < |\phi| \leq (\pi-\phi_0) \text{ or } \vartheta_0 < |\vartheta| \leq (\pi-\vartheta_0) \\ 0, & (\pi-\phi_0) < |\phi| \leq \pi \text{ or } (\pi-\vartheta_0) < |\vartheta| \leq \pi \end{cases}. \tag{4.15}$$

This approach is capable of dealing with closely spaced and highly correlated out-of-sector signals since it addresses the out-of-sector response. However, since this approach transforms the entire field of view for each of the sectors used it introduces a large transformation bias in the final estimates.

4.5 Proposed Approach

The approach proposed in this work is divided into various simple steps as shown in Figure 4.3. It aims to maximize the transformed region while keeping the transformation error within a predefined bound, to calculate an optimal subarray length for the Spatial Smoothing step, to achieve a proper estimation of the number of incoming signals and to perform a single DOA estimation and eliminate the sector-by-sector processing entirely.

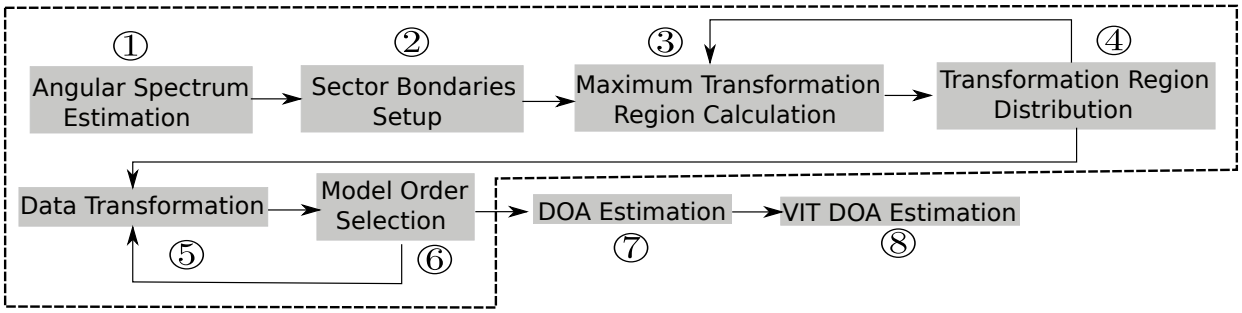

Figure 4.3: Flowchart of proposed approach

4.5.1 Angular Spectrum

One of the goals of the proposed array interpolation approach is to avoid the sector-by-sector processing entirely. Therefore the first step of the proposed approach is to obtain a first low resolution, computationally simple DOA estimation in order to address the correct regions of the field of view when calculating the transformation matrix. Since the array response needs to be known to construct $\mathbf{B}$, such knowledge can be used to detect angular regions where significant power is received. This estimation can be done with the conventional beamformer [12], yielding the normalized power response

$$P(\theta) = \frac{\mathbf{a}^{\mathrm{H}}(\theta)\hat{\mathbf{R}}_{\mathbf{XX}}\mathbf{a}(\theta)}{\mathbf{a}^{\mathrm{H}}(\theta)\mathbf{a}(\theta)} \in \mathbb{R}, \tag{4.16}$$

where $\hat{\mathbf{R}}_{\mathbf{XX}} = \frac{\mathbf{X}\mathbf{X}^{\mathrm{H}}}{N}$ is the estimate of the signal covariance matrix. In real systems the result of (4.16) is discrete in θ and can be written as

$$P[z] = P(-90^\circ + (z \cdot \Delta)) = P(\theta), \tag{4.17}$$

with $\theta \in \mathcal{D}_\Delta$where

$$\mathcal{D}_\Delta = [-90^\circ, -90^\circ + \Delta, ..., 90^\circ - \Delta, 90^\circ] \tag{4.18}$$

and Δ is the resolution of the azimuth angle of the power response (4.16).

Since the beamformer is only a delay and sum approach it is not affected by signal correlation and can provide low resolution estimates even in completely correlated signal environments. Although one could argue for using weighted beamformers such as the CAPON-MVDR [13] since this method offers increased resolution when compared the traditional beamformer it suffers in the

presence of highly correlated wavefronts in very high signal to noise ratio (SNR) and requires a matrix inversion, leading to a higher computational load. Therefore we employ the conventional beamformer in this first step due to its robustness and simplicity.

4.5.2 Sector Boundaries Setup

The next step is to decide based on the power spectrum which are the sectors of the array response that should be transformed. This can be done by scanning the output of (4.16) for sectors, and defining, for each sector, a respective lower bound $l_w \in \mathcal{D}_\Delta$ and upper bound $u_w \in \mathcal{D}_\Delta$ as shown in Figure 4.4. The threshold that defines a sector and its bounds can be defined, for

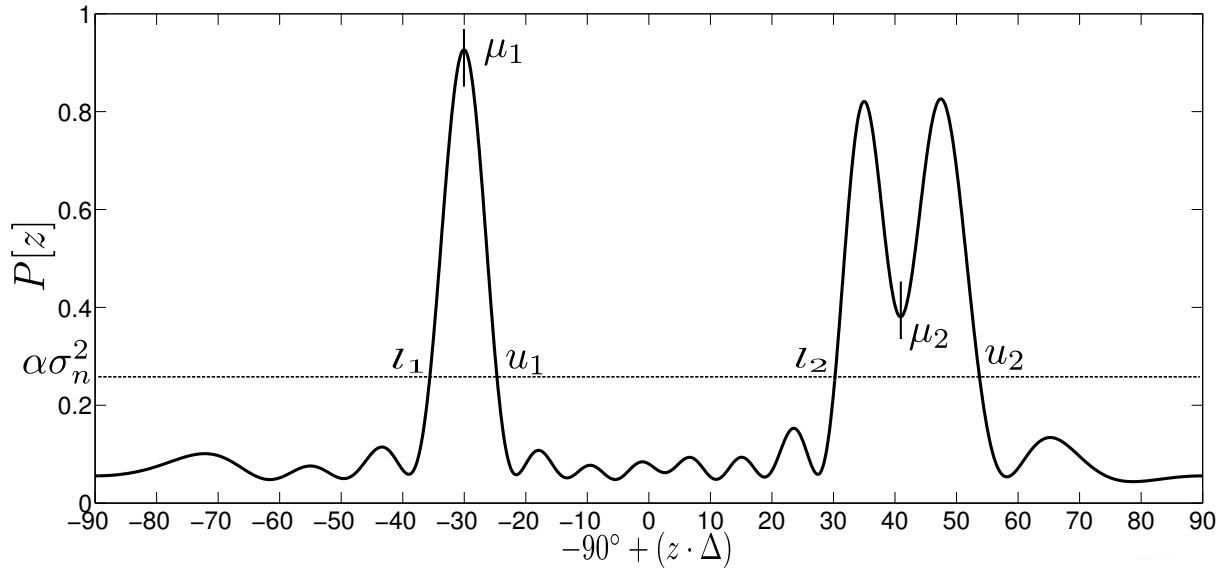

Figure 4.4: Selected sectors and respective bounds

instance, by looking at the noise power. The noise floor can be set at $\alpha\sigma_n^2$, with $\alpha > 1$ being a sensitivity parameter. A large α means that only large sectors are detected but coming at the cost of discarding smaller sectors that are related to a signal component, while a small α means that smaller sectors are detected but at the cost of allowing noise to be mistakenly detected as a sector. If W sectors are detected, a detected sector with bounds $[l_w, u_w]$ is said to be centered at

$$\mu_w = \left\lceil \frac{|u_w - l_w|}{2} \right\rfloor_{\mathcal{D}_\Delta} \in \mathcal{D}_\Delta, \tag{4.19}$$

where $\lceil \cdot \rfloor_{\mathcal{D}_\Delta}$ is a rounding operation to the domain $\mathcal{D}_\Delta$.

Peak search is not employed in this step since its more computationally expensive and could make the selection of upper and lower bound for a given peak a more complex process. For instance, in Figure 4.4 μ_2 is between two peaks that are not properly separated.

4.5.3 Maximum Transformation Region Calculation and Transformation Regions Distribution

The following two steps are dependent on each other and cannot be separated. The iterative approach presented here seeks to find out the maximum region of the field of view that can be transformed while keeping the transformation error bounded by a pre defined value. It also distributes the calculated region with respect the to power of each sector detected in the second step as shown in Subsection 4.5.2.

The first part of the next two steps is to calculate a weighting factor based on the power of each detected sector. This weighting factor will be used to optimally distribute the transformable region with respect to received power, focusing the transformation on regions with more power and aiming to leave the least significant power outside of the total transformed region. A weighting factor for each sector is calculated as

$$\xi_w = \frac{\sum_{z=l_w}^{u_w} P[z]}{\sum_{c=1}^{W} \sum_{z=l_c}^{u_c} P[z]} \in \mathbb{R}. \tag{4.20}$$

As mentioned in Section 4.4, classical array interpolation methods in the literature divide the array response into various sectors (sector-by-sector processing) in order to keep the error (4.9) small. However, in this work a single transform matrix is used based on a combination of the sectors detected in (4.16). In order to bound the error $\epsilon(\mathcal{S})$ a signal adaptive method for calculating the maximum transform size is used based on the weights calculated in (4.20). For a sector centered at μ_w, the discrete and countable set of angles used to transform this sector is given by

$$\mathcal{S}_w = \begin{cases} \left[\left\lceil \mu_w - \frac{\Xi\xi_w}{2} \right\rfloor_{\mathcal{D}_\Delta}, \left\lceil \mu_w - \frac{\Xi\xi_w}{2} + \Delta \right\rfloor_{\mathcal{D}_\Delta}, ..., \left\lceil \mu_k + \frac{\Xi\xi_w}{2} \right\rfloor_{\mathcal{D}_\Delta}\right] \\ \qquad\qquad\qquad\qquad\qquad\qquad , \Xi\xi_w < |u_w - l_w| \\ [l_w, l_w + \Delta, ..., u_w],\ \Xi\xi_w \geq |u_w - l_w| \end{cases} \tag{4.21}$$

and

$$\mathcal{S}_k \cap \mathcal{S}_{\bar{k}} = \emptyset \ \forall\ k, \bar{k} \in [1, ..., K] \text{ and } \mathrm{k} \neq \bar{\mathrm{k}}, \tag{4.22}$$

where $\Xi \in \mathbb{R}^+$ is the total transform size in degrees of all sectors. The combined sector is given by

$$\mathcal{S} = \mathcal{S}_1 \cup \mathcal{S}_2 \cup ... \cup \mathcal{S}_W. \tag{4.23}$$

Thus, $\mathcal{S}$ has a better resolution for the sectors $\mathcal{S}_w$ where more power is present (weighted by ξ_w), i.e the transformation of the combined sector $\mathcal{S}$ is weighted towards the sectors $\mathcal{S}_w$ that include more signal power as shown in Figure 4.5.

As the problem of obtaining the transform matrix $\mathbf{B}$ is equivalent to solving a highly overdetermined system we have

$$|\mathcal{S}| \to \infty \iff \epsilon(\mathcal{S}) \to \infty. \tag{4.24}$$

Thus, transforming the entire detected sectors may result in a very high transformation error introducing a very large bias into the final DOA estimates. To address this problem an upper

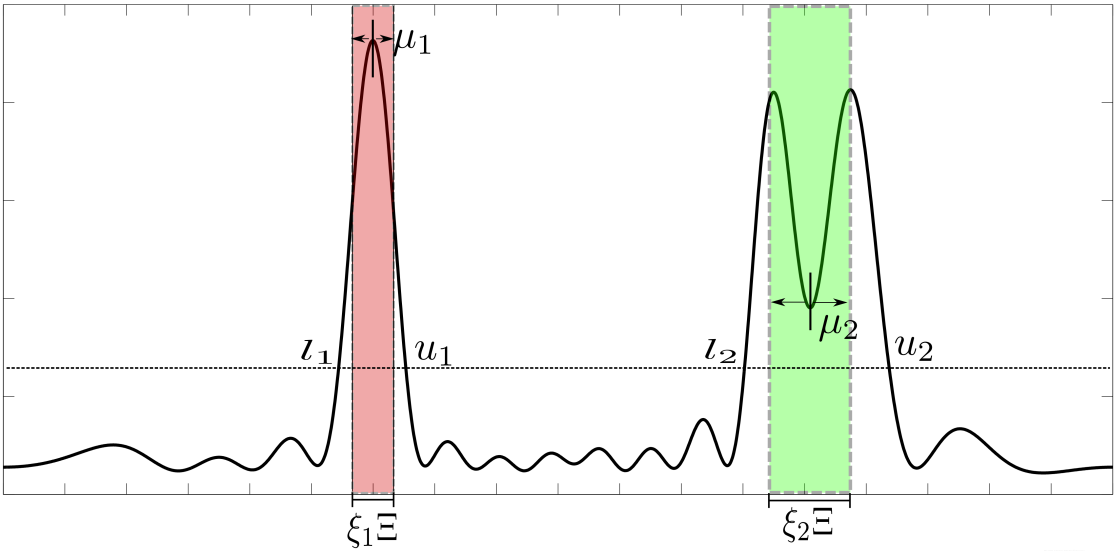

Figure 4.5: Example of transformed regions

bound to the transform error $\epsilon_{\max}$ needs to be defined and a search can be performed to find the maximum transform size covering the detected sectors that is still within the error upper bound. The problem of finding the maximum Ξ with respect to $\epsilon_{\max}$ can be written as the optimization problem

$$\max_{\Xi} \epsilon(\mathcal{S}) \tag{4.25}$$

$$\text{subject to } \epsilon(\mathcal{S}) \leq \epsilon_{\max} \tag{4.26}$$

$$\Xi \leq \Xi_{\max} = \sum_{k=1}^{K} |u_k - l_k| \tag{4.27}$$

$$\Xi \geq \Xi_{\min} = M\Delta. \tag{4.28}$$

The problem in (4.25), (4.26), (4.27), (4.28) can efficiently be solved using a bisection search method, since once all μ_w and ξ_w have been defined, the error function increases monotonically for $\Xi > \Xi_{\min}$, as illustrated in Figure 4.6. $\epsilon(\mathcal{S})$ is greatly affected if the calculation of $\mathbf{B}$ is either a heavily overdetermined or an underdetermined system. Therefore, $\Xi_{\min}$ is defined to ensure monotonicity of the problem given in (4.25).

In summation these two steps consist of calculating a set of transform matrices according to the weights given by (4.20) and looking for the maximum transform region that still yields a transformation errors bounded by $\epsilon_{\max}$.

4.5.4 Data Transformation and Model Order Selection

Once all μ_w and ξ_w as well as Ξ have been defined the final transformation matrix can be calculated. In order to obtain further insight into the calculation of the transformation matrix we

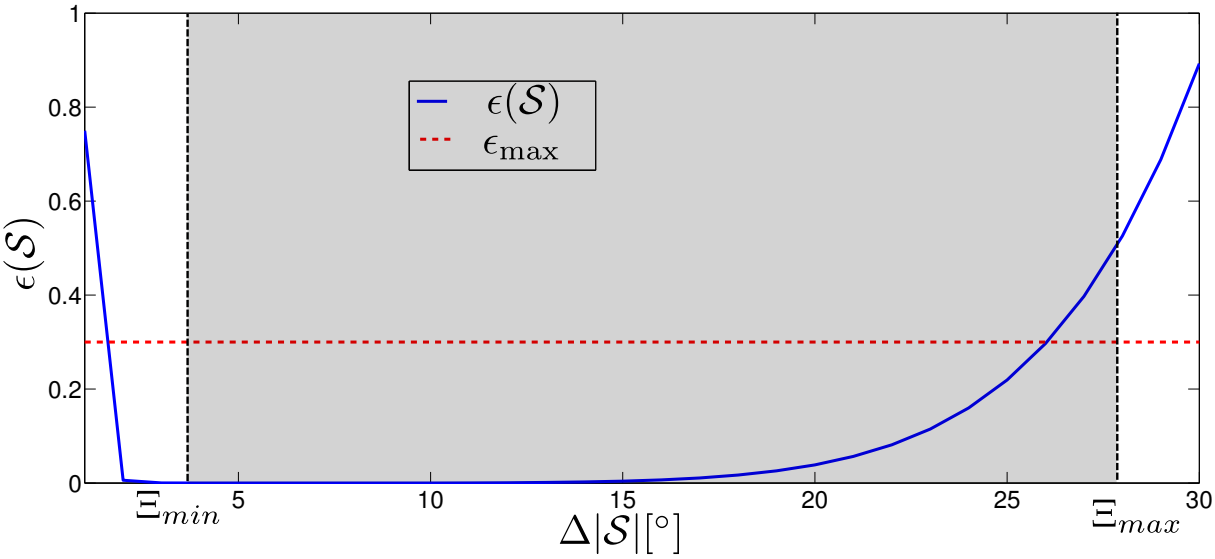

Figure 4.6: Transformation error with respect to combined sector size

now analyze (4.8) in detail

$$\begin{aligned}\mathbf{B} &= \bar{\mathbf{A}}\mathbf{A}^{\dagger} \\ &= \bar{\mathbf{A}}\mathbf{A}^{\mathrm{H}}(\mathbf{A}\mathbf{A}^{\mathrm{H}})^{-1} \\ &= \mathbf{R}_{\bar{\mathbf{A}}\mathbf{A}}{\mathbf{R}_{\mathbf{A}\mathbf{A}}}^{-1}.\end{aligned} \tag{4.29}$$

From (4.29) further insight into the calculation of the transformation matrix is available. The transformation matrix calculation can be seen as the transformation of the cross covariance between the real and desired array responses into the covariance of the desired array response if no errors are assumed. However, the desired array response covariance will be corrupted the noise present in the measurements, thus, taking such errors into account (4.29) can be rewritten as

$$\mathbf{B} = \mathbf{R}_{\bar{\mathbf{A}}\mathbf{A}}(\mathbf{R}_{\mathbf{A}\mathbf{A}} + \mathbf{B}\mathbf{R}_{\mathbf{N}\mathbf{N}}\mathbf{B}^{\mathrm{H}})^{-1}.$$

The noise present after transformation is colored by the transformation it self, therefore, the calculation of $\mathbf{B}$ will depend on $\mathbf{B}$ itself. To solve this problem a iterative approach can be used, $\mathbf{B}$ can be initialized using (4.8) and a new $\mathbf{B}$ can be obtained using this estimate, after that a new iteration of $\mathbf{B}$ is obtained using the previous value until convergence.

$$\begin{aligned}&\mathbf{B}_0 = \bar{\mathbf{A}}\mathbf{A}^{\dagger} \\ &\quad \text{for } i \geq 1 \\ &\mathbf{B}_i = \mathbf{R}_{\bar{\mathbf{A}}\mathbf{A}}(\mathbf{R}_{\mathbf{A}\mathbf{A}} + \mathbf{B}_{i-1}\mathbf{R}_{\mathbf{N}\mathbf{N}}\mathbf{B}_{i-1}^{\mathrm{H}})^{-1} \\ &\quad \text{repeat until convergence}\end{aligned}$$

Since $\mathbf{A}_{\mathcal{S}}$ is formed of closely spaced angular responses its column vectors are highly correlated, this high correlation leads to a suboptimal transformation. Thus, one can obtain a more statistically significant $\mathbf{B}$ by performing a reduced rank (RR) projection [40] that takes into account only the

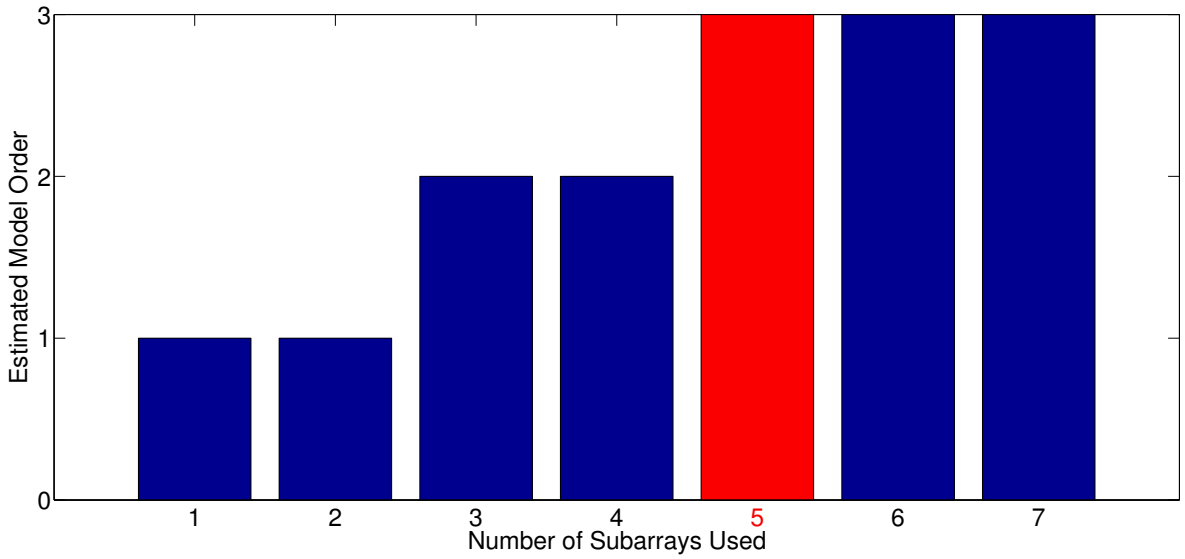

Figure 4.7: Example of estimated model order versus number of subarrays

principal components of $\mathbf{A}_{\mathcal{S}}$. Performing the singular value decomposition (SVD)

$$\mathbf{B}(\mathbf{A}_{\mathcal{S}} + \boldsymbol{\Upsilon}) = \mathbf{U}\mathbf{D}\mathbf{V}^{\mathrm{H}},$$

the singularvectors of $\mathbf{U}$ related to the r largest singularvalues are selected forming $\mathbf{U}_r \in \mathbb{C}^{M\times r}$ and the reduced rank $\mathbf{B}_r$ is given by the orthogonal projection

$$\mathbf{B}_r = (\mathbf{U}_r\mathbf{U}_r^{\mathrm{H}})\mathbf{B} \in \mathbb{C}^{M\times M}.$$

r can be selected using a model order selection scheme such as the RADOI [37].

Once $\mathbf{B}$ has been obtained, the transformed covariance including FBA and SPS is obtained by [16]

$$\bar{\mathbf{R}}_{\mathbf{XX}} = \frac{1}{2W}\sum_{w=1}^{W} \mathbf{J}_w^{\mathrm{T}}(\mathbf{B}\hat{\mathbf{R}}_{\mathbf{XX}}\mathbf{B}^{\mathrm{H}} + \mathbf{Q}\mathbf{B}\hat{\mathbf{R}}_{\mathbf{XX}}^{*}\mathbf{B}^{\mathrm{H}}\mathbf{Q})\mathbf{J}_w, \tag{4.30}$$

where $(\cdot)^*$ stands for the complex conjugation. While W can be chosen *a priori* it can also be adaptively chosen as to minimized the loss of effective array aperture while achieving a good estimate of L. We use as a model order estimation method $\mathrm{MOE}(\bar{\mathbf{R}}_{\mathbf{XX}}(W)) = \hat{L}$. Therefore we have to solve the problem

$$(W, \hat{L}) = \arg\min_{W}\max_{\hat{L}} \left\{\mathrm{MOE}(\bar{\mathbf{R}}_{\mathbf{XX}}(W))\right\}. \tag{4.31}$$

Figure 4.7 shows an example of selecting the optimal number of subarrays. After the maximum model order has been detected, increasing the number of subarrays offers no additional separation, since not extra signal was detected, and comes at the cost of sacrificing antenna aperture.

It is important to notice that the estimated number of impinging signals $\hat{L}$ can be different from the number of sectors detected in (4.16). Each of the detected sectors $\mathcal{S}_k$ can be formed by a set of nearly coherent signals that now can be efficiently separated with (4.31) allowing the

application of a high resolution DOA estimation method to jointly estimate the parameters of all the detected signals.

Its important the highlight now that if a maximum likelihood (ML) method [3, 4] or its extensions such as the expectation maximization (EM) [5, 6, 7, 8] or the space alternating generalized expectation maximization (SAGE) [9, 10] would be chosen for estimating the direction of arrival of the received signals the model order would have to be estimated first, and to do so, in highly correlated signal environments, FBA and SPS need to be applied since model order selection schemes rely on the analysis of the profile of the eigen or singular values. In practice, this means that even if a parametric ML method was to be used the steps taken so far into the algorithm would still need to be taken. Therefore, no claims of increased complexity can be made, up to this point, when the proposed DOA estimation algorithm is compared to a ML algorithm and the presented steps of proposed algorithm can be viewed as a separate part that can be applied to use ML methods in highly correlated signals, arbitrary geometry array environments if one has no prior knowledge of the number of received signals.

4.5.5 DOA Estimation

Once the number of signals has been estimated and with the FBA-SPS covariance matrix at hand a joint estimation of the DOAs of all the incoming signals can be performed. After FBA and SPS DOA estimation can be done with any DOA estimation method. For this work we choose the ESPRIT method since it is a closed form algorithm that can be very easily extended to multidimensional scenarios. It is important to highlight that the the current state of array interpolation in the literature [29] states that ESPRIT cannot be employed with a transformation matrix calculated as shown previously in this work. Thus, although this section does not present any new method for DOA estimation it is still novel to apply ESPRIT to a transformation matrix applied directly to the signal covariance matrix.

The ESPRIT parameter estimation technique is based on subspace decomposition. Matrix subspace decomposition is usually done by applying the Singular Value Decomposition (SVD). The SVD of the matrix $\mathbf{X} \in \mathbb{C}^{M \times N}$ is given by

$$\mathbf{X} = \mathbf{U}\mathbf{\Lambda}\mathbf{V}^{\mathrm{H}}, \tag{4.32}$$

where $\mathbf{U} \in \mathbb{C}^{M \times M}$ and $\mathbf{V}^{N \times N}$ are unitary matrices called the left-singular vectors and right-singular vectors of $\mathbf{X}$ and $\mathbf{\Lambda} \in \mathbb{C}^{M \times N}$ is pseudo diagonal matrix containing the singular values of $\mathbf{X}$. The signal subspace $\mathbf{E}_S \in \mathbb{C}^{M \times \hat{L}}$ of $\mathbf{X}$ can be constructed by selecting only the singular vectors related to the $\hat{L}$ largest singular values, the remaining singular vectors form the noise subspace $\mathbf{E}_N \in \mathbb{C}^{M \times M - \hat{L}}$ of $\mathbf{X}$.

Equivalently eigenvalue decomposition can be applied on the auto correlation matrix $\hat{\mathbf{R}}_{\mathbf{XX}}$ of $\mathbf{X}$ spanning the same subspace

$$\hat{\mathbf{R}}_{\mathbf{XX}} = \mathbf{E}\mathbf{\Sigma}\mathbf{E}^{-1}, \tag{4.33}$$

where $\mathbf{E} \in \mathbb{C}^{M \times M}$ and $\mathbf{\Sigma} \in \mathbb{C}^{M \times M}$ contains the eigenvectors and eigenvalues of $\mathbf{R}_{\mathbf{XX}}$. The eigenvectors related to the $\hat{L}$ largest eigenvalues span the same signal subspace $\mathbf{E}_S$ of the single

value decomposition. The same holds for the noise subspace of the EVD and left singular vectors of the SVD, $\mathbf{E}_N$.

This classic eigendecomposition is suitable when the noise received at the antenna array is spatially white, since, in our case, we apply a transformation to the data, even if the received noise was originally white it turns in colored noise. To deal with colored noise the generalized eigenvalue decomposition (GEVD) can be used to take the noise correlation into account, the GEVD of the matrix pair $\bar{\mathbf{R}}_{\mathbf{XX}}$, $\bar{\mathbf{R}}_{\mathbf{NN}}$ is given by

$$\bar{\mathbf{R}}_{\mathbf{XX}}\bar{\mathbf{\Gamma}} = \bar{\mathbf{R}}_{\mathbf{NN}}\bar{\mathbf{\Gamma}}\mathbf{\Lambda}, \tag{4.34}$$

where $\mathcal{E} \in \mathbb{C}^{M\times M}$ is a matrix containing the generalized eigenvectors and $\mathbf{\Lambda} \in \mathbb{R}^{M\times M}$ is a matrix containing the generalized eigenvalues in its diagonal. Notice that this decomposition is the same as the EVD (4.33) for $\bar{\mathbf{R}}_{\mathbf{NN}} = \mathbf{I}$. The subspace $\bar{\mathbf{\Gamma}}_S \in \mathbb{C}^{M\times \hat{L}}$ is formed selecting the generalized eigenvectors related to the $\hat{L}$ largest generalized eigenvalues. This subspace, however, does not span the same column subspace as the original steering matrix, and needs to be reprojected onto the original manifold subspace or dewhitened. This can be done by

$$\mathbf{\Gamma}_s = \bar{\mathbf{R}}_{\mathbf{NN}}\bar{\mathbf{\Gamma}}_s. \tag{4.35}$$

With this subspace estimate at hand the Total Least Squares (TLS) ESPRIT [22] is applied. Two subsets of the signal subspace that are related trough the shift invariance property need to be selected. The choice depends on with parameter is to be estimated and are directly dependent on the way the data has been organized. For the signal model shown in 3.10 if one wanted to estimate the direction of arrival one could select the first $M-2$ rows of the signal subspace as the first subset and the last $M-2$ rows as the last subset, if, on the other hand, the polarization parameter is to be estimated, one could select the rows of odd index as its first subset and the rows of even index as the second subset. Figure 4.8 shows an example for a rectangular array with dual polarization, in the figure black and gray circles represent antennas with different polarizations. The TLS-ESPRIT algorithm presented does not depend on subset selection, and will be presented in a general way.

Let $\mathbf{\Gamma}_1$ and $\mathbf{\Gamma}_2$ represent the subspace subsets selected in as previously mentioned. A matrix $\mathbf{\Gamma}_{1,2}$ is constructed as

$$\mathbf{\Gamma}_{1,2} = \begin{bmatrix} \mathbf{\Gamma}_1^{\mathrm{H}} \\ \mathbf{\Gamma}_2^{\mathrm{H}} \end{bmatrix} [\mathbf{\Gamma}_1\mathbf{\Gamma}_2], \tag{4.36}$$

by performing and eigendecomposition of $\mathbf{\Gamma}_{1,2}$ and ordering its eigenvalues in the decreasing order and its eigenvectors accordingly the eigenvector matrix $\mathbf{V}$ can be divided into blocks as

$$\mathbf{V} = \begin{bmatrix} \mathbf{V}_{1,1} & \mathbf{V}_{1,2} \\ \mathbf{V}_{2,1} & \mathbf{V}_{2,2} \end{bmatrix}. \tag{4.37}$$

Finally, the parameters can be obtained by finding the eigenvalues of

$$\Phi = \mathrm{eig}\left(-\frac{\mathbf{V}_{1,2}}{\mathbf{V}_{2,2}}\right). \tag{4.38}$$

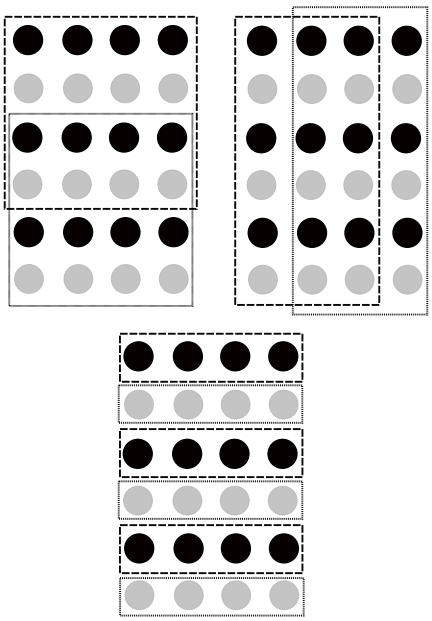

Figure 4.8: Example of select subsets

The parameters in Φ can represent a phase delay respective to a direction of arrival if DOAs are being estimated, or can represent the ratio of the strength at which a signal appears in the different polarizations.

For multidimensional arrays another option is to employ methods based on the PARAFAC decomposition such as [41], [42] instead of the ESPRIT.

4.6 Vandermonde Invariance Transformation

Finally, once the first set of estimates has been obtained the Vandermonde Invariance Transformation (VIT) can be applied, this transformation aims to shape the noise alway from the regions where the signal is arriving in order to obtain improved estimates [31] . The VIT is an array interpolation approach that transforms a vandermonde system with a response linear with respect to the angle of arrival into an also vandermonde system with a highly nonlinear response with respect to the angle of arrival. The VIT promotes a nonlinear transformation with respect to the selected spatial frequency $\mu(\phi)$. Let $\mathbf{u} = [1, \mathrm{e}^{\mathrm{j}\mu(\phi)}, \ldots, \mathrm{e}^{\mathrm{j}\mu(\phi)(\mathrm{M}-1)}]$, the VIT performs the following transformation

$$\bar{\mathbf{u}}^{(VIT)} = \mathbf{T}(\phi)\mathbf{u} = \left(\frac{\mathrm{e}^{\mathrm{j}\mu(\phi)} - r}{1 - r}\right) \begin{pmatrix} 1 \\ e^{\mathrm{j}\nu(\phi)} \\ \vdots \\ e^{\mathrm{j}\nu(\phi)(M-1)} \end{pmatrix}, \tag{4.39}$$

r and ν are design parameters that can be chosen considering a compromise between the level of noise suppression desired around μ and the linearity of the output.

The VIT can be used to apply a phase attenuation to the dataset, which in turn shapes the noise,

reducing the power of the noise in the region near $\mu(\phi)$ and increasing it over its vicinity. Thus, the VIT needs to be applied angle wise, i.e, a set of initial estimates of the angles ϕ is used to calculate a VIT centered over the given angles, and a second estimate is performed. This second estimation yields and offset ϕ_{offset} with respect to the original ϕ, giving the final estimation $\phi_{\text{VIT}} = \phi + \phi_{\text{offset}}$. Due to the mentioned noise shaping, this final estimation offers increased precision, but comes at the cost of transforming the dataset and applying the chosen DOA estimation method $\hat{L}$ times.

The VIT can be interpreted as a zoom, similar to an optical zoom, with the first estimates a zoom can be used on the regions of the manifold where signal has been estimated to arrive and the region can be inspected with the zoom effect to detect any imprecisions from the first estimate. The increased performance comes at the cost of $\hat{L}$ extra DOA estimations.

4.7 Numerical Simulations

To test the efficiency of the proposed approach a set of numerical simulations is performed and results are compared to the Cramér–Rao bound (CRB) for the true array response and compared to the current state-of-the-art approach proposed in [24]. In Subsection 4.7.1 the performance of the proposed method is studied in the presence of spatially white Gaussian noise. In Subsection 4.7.2 the case where the measurement data of the array response contains errors is studied.

4.7.1 Performance in the presence of white noise

The array response assumed in the simulations shown in Figure 4.9 is constructed by randomly displacing the elements of a Uniform Linear Array (ULA) composed of $M = 8$ antennas with inner element spacing of $\frac{\lambda}{2}$ to a point belonging to a circle with center on the original antenna position and radius $\frac{0.1\lambda}{2}$, where λ is the wavelength of the carrier frequency of the signal. For obtaining $\hat{\mathbf{R}}_{\mathbf{XX}}$ we use $N = 200$ snapshots and the Root Mean Squared Error (RMSE) is calculated with respect to 1000 Mont Carlo simulations. Three signals impinging from $\phi_1 = 45°$, $\phi_2 = 38°$ and $\phi_3 = 15°$ with $\sigma_1^2 = \sigma_2^2 = \sigma_3^2 = 1$ and $\rho_{1,2} = 1$, $\rho_{2,3} = \rho_{1,3} = 0.8$ according to equation (3.25) are impinging on the array. The Signal to Noise Ratio (SNR) is defined as

$$\text{SNR} = \frac{\sigma_1^2}{\sigma_{\text{n}}^2} = \frac{\sigma_2^2}{\sigma_{\text{n}}^2} = \frac{\sigma_3^2}{\sigma_{\text{n}}^2}. \tag{4.40}$$

In Figures 4.9 and 4.11 the given RMSE is

$$\text{RMSE} = (\sqrt{(\phi_1 - \hat{\phi}_1)^{\mathbf{2}} + (\phi_2 - \hat{\phi}_2)^{\mathbf{2}} + (\phi_3 - \hat{\phi}_3)^{\mathbf{2}}})/3, \tag{4.41}$$

where $\hat{\theta}_i$ is the estimate of θ_i. The CRB shown in Figure 4.9 is the sum CRB for all estimated DOAs. The two parameters that fully define the proposed approach given are set to $\alpha = 1.2$ and $\epsilon_{\max} = 10^{-3}$.

In [24] a sector-by-sector processing with out-of-sector response filtering and applying MUSIC is proposed. We use the same approach for the calculation of the transformation matrices as given in [24] while additionally applying FBA and SPS as well as using Root-MUSIC instead of MUSIC.

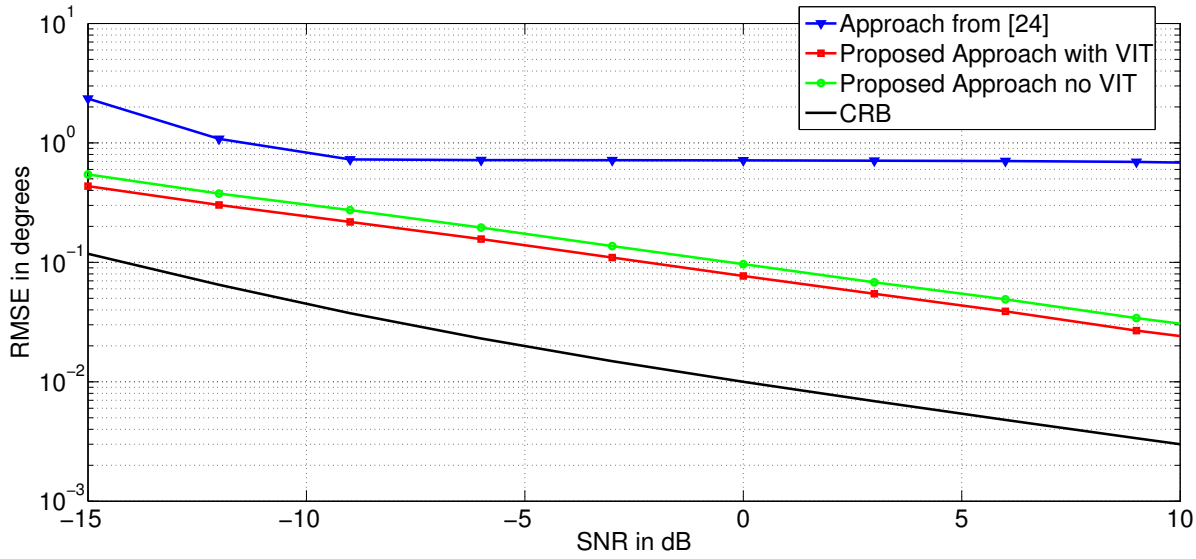

Figure 4.9: RMSE for [24] and proposed approach with and without the VIT

Furthermore, we assumed, for the simulations of the approach given in [24] that the model order is perfectly known. Figure 4.9 shows that while the estimates provided by the approach of [24] with Root-MUSIC are reasonably precise, the error is less than one degree for a moderate SNR, it quickly reach a plateau for this demanding signal scenario as the DOA estimation bias is dominated by large transformation errors for each sector since for each sector the approach of [24] transforms the entire filed of view of the array.

On the other hand, the approach proposed in this work provides improved accuracy with increasing SNR since the size of the combined sector also decreases, resulting in a much smaller transformation error. The proposed approach is still not capable of reaching the CRB due to the application of SPS, which effectively decreases array aperture, however, W being chosen according to (4.31). The proposed approach also does not assume a known model order. It is possible to see that the proposed VIT step is capable of producing estimates that are, in average, 2 dB better than the original estimates.

As a figure of merit we compare the performance of Root-MUSIC and ESPRIT for a perfect ULA without array transformation and with no correlation between the three signals. As shown in Figure 4.10 the performance of Root-MUSIC and ESPRIT is very similar in the absence of array imperfections and correlated signals, hence the performance increase shown in Figure 4.9 is due to the proposed array interpolation method and not to the mere usage of the ESPRIT algorithm.

4.7.2 Robustness to Errors in the Array Response Model

In reality the true array response is not fully known and can only be derived by empirical measurements which include measurement errors. To study a scenario where the measurements data of the array response are corrupted by measurement errors we introduce additional positioning errors. We consider the same signal scenario as in Section 4.7.1 while the SNR for this set of

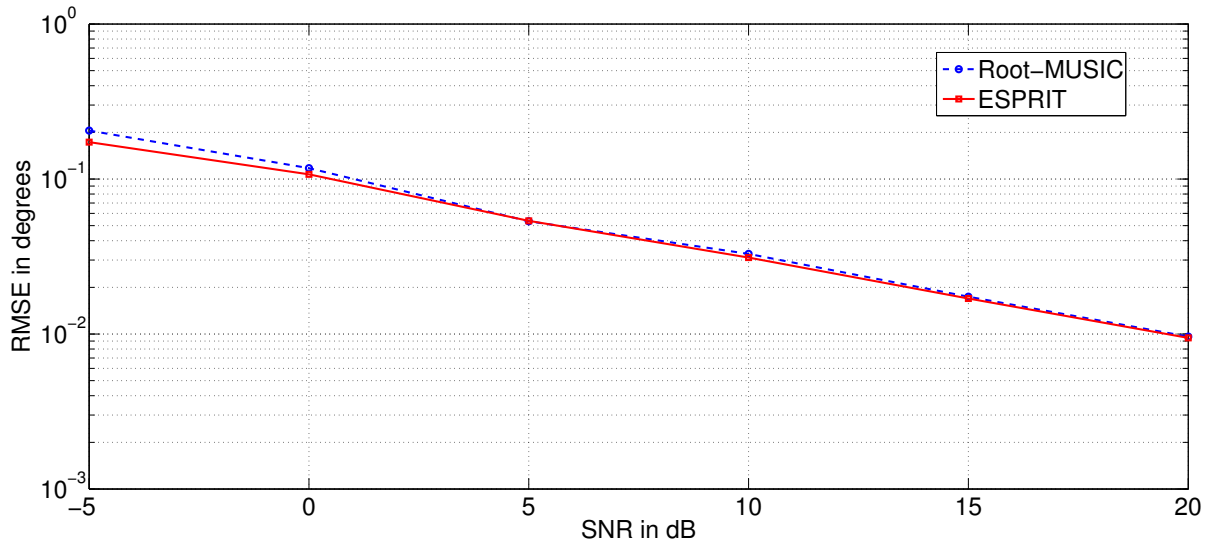

Figure 4.10: Performance of Root-MUSIC versus ESPRIT

simulations is kept fixed at 15 dB and the variance σ_e^2 of the additional errors are given in fractions of $\frac{\lambda}{2}$ and range from 0.02 to 0.2.

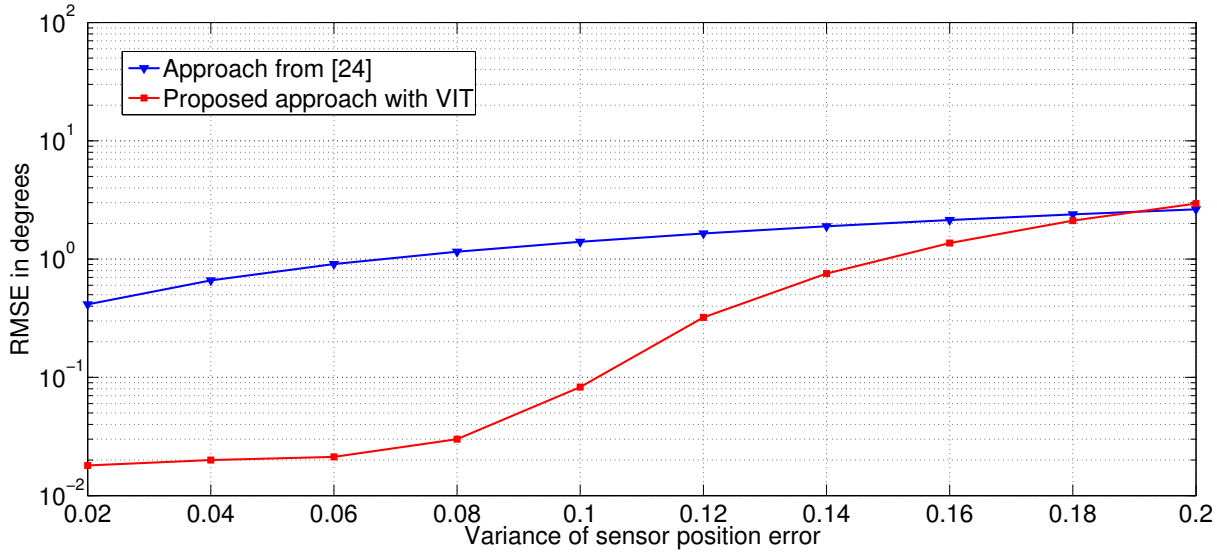

Figure 4.11: RMSE with array response model errors

Figure 4.11 shows that the proposed approach provides improved accuracy for errors drawn from $\mathcal{N}(0, \sigma_e^2 < 0.2)$. Since the proposed approach relies on the shift invariance of the array, arrays with large unknown positioning errors (errors of empirical measurements) are not correctly transformed into shift invariant arrays, thus, resulting in large inaccuracies in the final estimations.

4.8 Summary

In this chapter a novel array interpolation approach has was presented. The approach addressed the main problems of the current state-of-the-art approaches present in the literature, avoiding entirely the sector-by-sector processing using a single sector focused on all regions with received signal. The model order can be estimated without any major problems since no signal is left outside of the transformation. The single sector used allows for a single joint DOA estimation, avoiding entirely the problems of selecting real estimates. The proposed approach was shown to achieve improved results when compared to the state-of-the-art approach currently available and shown to be robust to errors in to knowledge of the true array response. The proposed approach is extremely flexible and can be used for a very large number of different applications as shown in Chapter 5.

Chapter 5

Applications

5.1 Global Navigation Satellite Systems Receiver with an Antenna Array

Global Navigation Satellite Systems (GNSS) are currently an important part of the day to day routine of many. GNSS receivers are present in cellphones, watches and computers for a variety of reasons, from standard street navigation to device tracking. While the current accuracy and reliability of GNSS systems is enough for the day to day use of the average person, there is no grave treat in losing GNSS tracking while one navigates the streets of an unknown city, it still hinders the application of GNSS systems for some sensible applications. A large number of recent military systems operate using the GNSS systems, automatic guided weapons, however, only rely on GNSS systems to correctly set a reference for the internal Inertial Measurement Units (IMUs) such as accelerometers and gyroscopes, even thought these units present drift errors [43], [44]. This is due to the current lack of robustness of GNSS receivers, even military grade receivers, to jamming or spoofing. Also, safety of life applications, such as automated control of aircrafts, require a very high precision that cannot be guaranteed on current GNSS receivers. In this section we present a framework for producing jamming and spoofing resistant receivers that are capable of providing improved precision based on the array interpolation framework presented on Chapter 4.

The main objective of the proposed approach is to calculate the time delay of arrival (TDOA) of a line of sight (LOS) signal from a GNSS satellite with high precision and while receiving a number of close multipath copies or non line of sight (NLOS) components, jamming and spoofing, modeled as highly correlated copies of the LOS signal.

5.1.1 Satellite Separation

First in ① the signals from each satellite are separated from each other by applying a bank of PR code matched correlators. In GPS signals signals are transmitted using the spread spectrum, with each satellite possessing a so called gold code or PR sequence, a binary sequence that is quasi-orthogonal to the sequences of the remaining satellites. Each sequence is composed of 1023

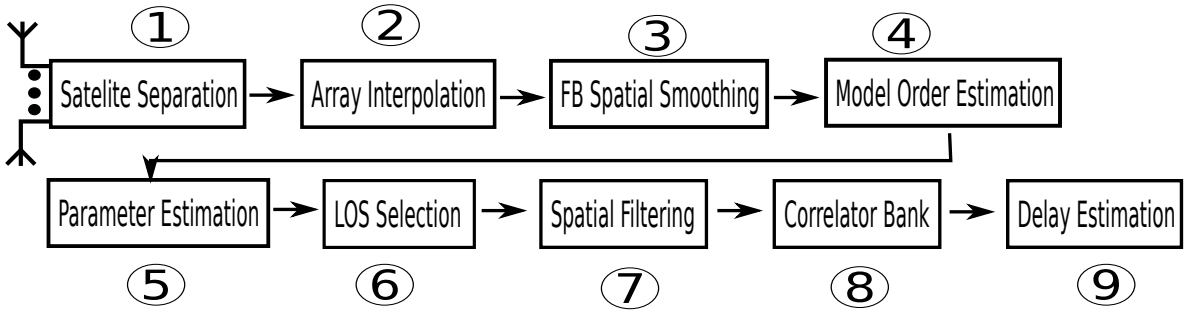

Figure 5.1: Block diagram of the proposed system

bits, known as chips. Satellite separation can be easily performed by correlating (multiplying and integrating) the received signal with the PR sequence of each satellite. Let $\mathbf{x}_{m_1,m_2}[k] \in \mathbb{C}^{N\times 1}$ denote the sampled signal at sensor m_1, m_2 during the k-th period of the observation interval and $\mathbf{pr}_{sat} \in \mathbb{C}^{N\times 1}$ be a vector contained the PR sequence binary code used by satellite sat, note that in that case that $N > 1023 \cdot F_s$, where F_s is the sampling frequency, the elements of $\mathbf{pr}_{sat}$ are periodic with period $1023F_s$. The satellite separated signal $\bar{\mathbf{x}}_{m_1,m_2} \in \mathbb{C}^{1\times \frac{N}{T_i}}$ is given by

$$\bar{\mathbf{x}}_{m_1,m_2}[j+1] = \sum_{i=1}^{T_i} \mathbf{x}_{m_1,m_2}[jT_i + i]\mathbf{pr}_{sat}[jT_i + i] \tag{5.1}$$

for $j = 0, 1, 2, ..., \frac{N}{T_i} - 1$, where T_i denotes the integration period, or the number of samples that will be summed in this preprocessing step. Since the correlation of $\mathbf{pr}_{sat_1}$and $\mathbf{pr}_{sat_2}$ is approximately zero for $sat_1 \neq sat_2$ the signal related to sat_1 rises accordingly to the choice of T_i while signals related to other satellites are all but eliminated. Another advantage of this step is reducing the interference caused the elements of $\mathbf{B}[k]$, since spurious interfering signals are not expected to have a high correlation with the PR sequence. This step is very important in order to reduce overall system complexity, since dealing with a very large number of signals would demand a very large number of antennas, making the proposed system not usable for real life implementations. Assuming that the noise has no correlation with the PR sequences it is easy to notice that the integration rises the power level of the signal matched to the PR sequence while keeping the power level of the noise constant, this is specially important in GNSS applications, where the original samples signal is bellow the noise floor with usual SNRs ranging from -20dB to -35dB. This low SNR is actually very useful, since the noise correlation can be measured prior to correlation, allowing for a very good estimate of noise correlation. There is, however, a tradeoff between T_i and the ability of the system to operate online on fast moving receivers. As the integration period rises the number of samples available at a fixed time period decreases making online estimation for fast moving receivers impractical for a T_i too large, this tradeoff needs to be taken into consideration and is application dependent.

5.1.2 Parameter Estimation

Steps ②, ③, ④ and ⑤ are done according to the method presented on Chapter 4.

5.1.3 Line of Sight Selection

At the end of step ⑤ we have a set of parameters for each estimated signal. Assuming a rectangular array with dual polarization we have azimuth, elevation and the ratio between the signals received at the RHCP and LHCP antennas. The first step is to discard the estimates that come from regions of the manifold where a satellite could not possibly be located, jammers and spoofers will usually be located on the ground, thus, given the placement of the antenna array, signals that do not arrive from a region feasible for a satellite signals can be discarded. If a jammer or spoofer would be located on a high altitude airplane, such airplane would be moving much faster in relation to the receiver than a satellite, and thus, by looking into the Doppler shift this kinds of jammers and spoofers can be discarded also. If the interferer has prior knowledge of the location of the receiver and can compensate for the Doppler shift the rate at which the DOA of the interferer is changing can be looked at to distinguish it from real satellite signals. Signals from the GNSS system are RHCP, thus, from the candidates left after the previous steps the LOS can be selected as the one with the largest RHCP to LHCP ratio.

5.1.4 Spatial Filtering

After the LOS signal has been selected a spatial filter can be applied. The idea is to filter the signals received from all the other directions leaving only the LOS signal. This can be done by using a delay and sum method

$$\mathbf{x}_{\text{los}} = [\mathbf{a}(\phi_{los}, \vartheta_{los}) \otimes \mathbf{u}(\phi_{\text{los}}, \vartheta_{los})]^{\text{H}}\mathbf{X} \in \mathbb{C}^{1\times N}. \tag{5.2}$$

$\mathbf{x}_{\text{los}}$ is a vector containing the symbols received only from the directions ϕ_{los} and ϑ_{los}. It is important to notice that this is applied directly to the received signal and not to the satellite separated version of the signal.

5.1.5 Correlator Bank

The next step is to put the signal $\mathbf{x}_{\text{los}}$ trough a correlator bank matched to different delays of the PR sequence within one chip. This process is very similar to what is done in ① but instead of using different PR sequences shifted versions of the same PR sequence are used. Assuming a correlator matched to five different delays, the output of a correlator *cor* matched to a delay PR sequence $\mathbf{pr}_{\text{cor}}$ is given by

$$\mathbf{y}_{cor}[j+1] = \sum_{i=1}^{T_i} \mathbf{x}_{\text{los}}[jT_i + i]\mathbf{pr}_{\text{cor}}[jT_i + i], \tag{5.3}$$

the vectors $\mathbf{y}_{cor}$ for the different delay matched correlators are arranged in the columns of the matrix matrix

$$\mathbf{Y} \in \mathbb{C}^{C\times\frac{N}{T_i}}, \tag{5.4}$$

where C is the number of delayed PR sequences used.

5.1.6 Delay Estimation

Finally, the TDOA of the LOS signal can be estimated. This estimation can be done by extending the MUSIC concept to the delay domain. First, we obtain the covariance matrix of the output of the correlator

$$\mathbf{R_{YY}} = \frac{\mathbf{Y}\mathbf{Y}^{\mathrm{H}}}{\frac{N}{T_i}}. \tag{5.5}$$

We then perform the eigenvalue decomposition of $\mathbf{R_{YY}}$

$$\mathbf{R_{YY}} = \mathbf{\Omega}\mathbf{\Upsilon}\mathbf{\Omega}^{-1}. \tag{5.6}$$

Since now we have properly isolated the LOS signal related to the satellite of interest the noise subspace $\mathbf{\Omega}_n$ can be constructed by removing from $\mathbf{\Omega}$ the eigenvector related to the largest eigenvalue. The delay can then be estimated by looking for peaks in

$$P(\tau) = \frac{\mathbf{c}(\tau) \times \mathbf{c}(\tau)^{\mathrm{H}}}{\mathbf{c}(\tau)^{\mathrm{H}} \times \mathbf{\Omega}_n \times \mathbf{\Omega}_n^{\mathrm{H}} \times \mathbf{c}(\tau)}, \tag{5.7}$$

where $\mathbf{c}(\tau)$ is the cross correlation between a signal that would be received with a given delay τ and the bank of correlators. The result is a delay spectrum as shown in Figure 5.2.

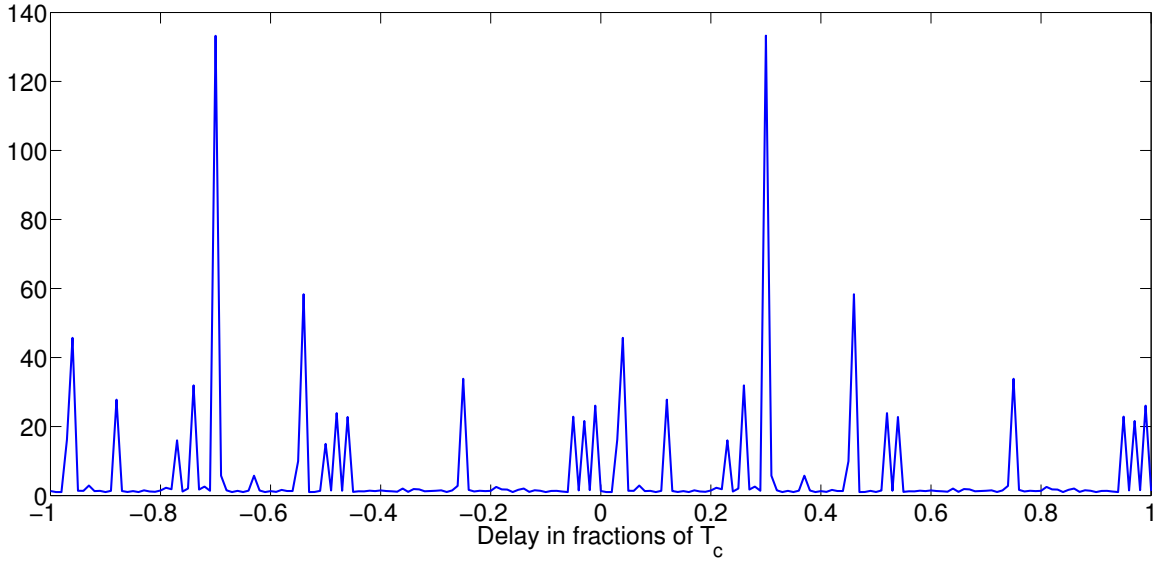

Figure 5.2: Example of delay spectrum

The estimated TDOA can be found by looking for peaks in the delay spectrum. Notice from Figure 5.2 that the spectrum is symmetric with respect to a 1 T_C delay difference, since this is the period of the PR sequence it is impossible to tell if a signal has a delay $-T_C$ or $+T_C$ by looking only at the delay spectrum. Assuming the GNSS system is running is steady state this can be solved by the DLL or PLL used for phase tracking.

5.2 Wireless Sensor Networks as Antenna Arrays

In recent years wireless sensor networks have been employed in a large number of applications. Their usage ranges from military applications, such battlefield surveillance and targeting, to health applications, such as automating drug applications in hospitals [45]. Some of these applications, battlefield surveillance for instance, require the positions of the sensors to be known across the network either in a relative or absolute manner. Since sensors can be deployed in a random manner an automatic method of sensor location is required.

Absolute positioning can be integrated to nodes by equipping each node with a Global Navigation Satellite Systems (GNSS) module such as a Global Positioning System (GPS) module. However, most WSNs are composed of highly simple hardware and also posses a highly limited energy budget, thus making this alternative impractical or even impossible. Employing GNSS also results in a network that is no longer self contained, as it relies on the presence of an external system to properly function.

A large number of alternatives have been proposed for relative sensor localization. One of the simplest ones is estimating the distance between nodes by measuring the power of a received signal, this approach requires a very precise model of signal attenuation which may be hard to obtain [46] and a fairly stable operation environment.

Another proposed method is by measuring the number of times a packet needs to be retransmitted in order to reach a given destination. The Radio Hop Count [47] is capable of providing a relative localization across the network without the presence of additional hardware and with a better precision than the RSSI method.

Some methods rely on analyzing the difference between the data measured by each sensor and trying to fit the measured data to a given positioning model. In [48] the sounds measured by a network of microphones are used in order to estimate the positions of the sensors in the environment.

In this work we present an alternative to sensor localization using DOA estimation. Instead of relying on antenna arrays we employ only a single crossed dipole antenna, extending the work seen in [49] to a simpler scenario. After the localization has been acquired the array interpolation proposed in Chapter 4 can be used to transform the sensor network into an effective antenna array.

5.2.1 Problem Description

We assume a network formed consisting of K sensors randomly placed at points $S_1, S_2, ..., S_K$ where

$$S_1 = [x_1, y_1]. \tag{5.8}$$

We also assume the presence of a set of nodes $S_i, ..., S_j$ that posses prior information about their own localization in the network. The proposed method requires

$$|i, ..., j| \geq 3. \tag{5.9}$$

It is also assumed that the orientation of all sensors in know with respect to a common reference, this can be done by employing a beacon transmitter or assuming an internal compass is present.

5.2.2 Polarization Model

The electric field of a propagating wave can be presented as

$$E = -E_x \mathbf{e}_x + E_y \mathbf{e}_y, \tag{5.10}$$

where E_x and E_y are the horizontal and vertical components of the electric field. These components define a polarization ellipse shown in Figure 5.3.

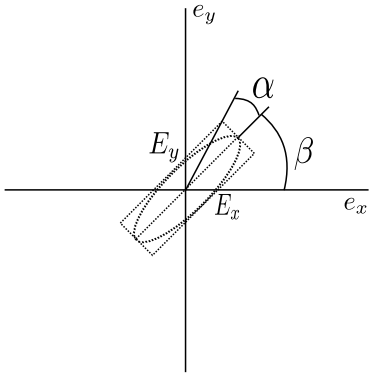

Figure 5.3: Polarization ellipse

Note that the electric field components can be written now in terms of the electric angles α and β as

$$E_x = E\cos(\gamma) \tag{5.11}$$
$$E_y = E\sin(\gamma)\mathrm{e}^{j\eta} \tag{5.12}$$

where

$$\cos(2\gamma) = \cos(2\alpha)\cos(2\beta) \tag{5.13}$$
$$\tan(\eta) = \tan(2\alpha)\csc(2\beta). \tag{5.14}$$

Considering a wavefront impinging over a crossed dipole with components parallel to the $x-$ and $y-$ axis of the polarization ellipse the output at such dipoles will be proportional to the components E_x and E_y respectively and be written as

$$\begin{aligned} E &= (-E_x)\mathbf{e}_x + (E_y\cos(\theta))\mathbf{e}_y \\ &= -\cos(\gamma)\mathbf{e}_x + \sin(\gamma)\cos(\theta)\mathrm{e}^{j\eta}\mathbf{e}_y \end{aligned} \tag{5.15}$$

where θ is the angle of arrival of the received wave with respect to the $x-$ axis.

The received signal can now be expressed in matrix as

$$\mathbf{X} = \mathbf{us} + \mathbf{N} \tag{5.16}$$

where $\mathbf{X} \in \mathbb{C}^{2\times N}$ is the matrix containing the measured outputs at each of the dipoles, N is the number of measured snapshots, $\mathbf{s} \in \mathbb{C}^{1\times N}$ is the vector contain the original transmitted signal transmitted, $\mathbf{N} \in \mathbb{C}^{2\times N}$ is the matrix containing the Additive White Gaussian noise present at sampling and the vector $\mathbf{u} \in \mathbb{C}^{2\times 1}$ is defined as

$$\mathbf{u} = \begin{bmatrix} -\cos(\gamma) \\ \sin(\gamma)\cos(\theta)\mathrm{e}^{j\eta} \end{bmatrix}. \tag{5.17}$$

5.2.3 Sensor Localization

The approach proposed in this work consists of analyzing the ratio between the outputs of the crossed dipole in order to estimate the direction of arrival of the received signal. Given the ratio

$$r = \frac{-\cos(\gamma)}{\sin(\gamma)\cos(\theta)\mathrm{e}^{j\eta}}, \tag{5.18}$$

the angle θ can be obtained by

$$\theta = \cos^{-1}\left(\frac{-\cos(\gamma)}{r\sin(\gamma)\mathrm{e}^{j\eta}}\right). \tag{5.19}$$

One way to estimate the ratios is to simply average a large number of samples from both antennas in order to reduce the effects of the noise and obtain the ratio between the powers. It is important to highlight at this point that although there is a need for a crossed dipole with two independent outputs to be present it is not necessary that both outputs are connect to individual receiver radios. A single symbol can be measured at both outputs by dividing the symbol duration, assuming the transmitted energy is constant over the entire symbol duration.

A more precise approach is to employ the ESPRIT algorithm presented in Section 4.5.5 in order to obtain the ratio between the received symbols. The advantage of the ESPRIT algorithm is that it is capable of dealing much more efficiently with noise since it relies on an eigendecomposition that separates noise and signal subspaces.

Although the ESPRIT method is capable of obtaining much more precise estimates as shown in Figure 5.4 it generates a larger computational load. This load is, however, justified as a small error in the estimated ratio may lead to a large error in the estimation of the DOA. This computationally demanding step is also only necessary once every time the topology of the network changes, thus, the ratio at which sensors change location needs to be taken into account when choosing the estimation method.

Note that the DOA is given with respect to the reference of the $\mathbf{x}-$axis and cannot distinguish from with direction, front or rear, the signal is arriving. Figure 5.5 displays this phenomenon.

Observe from Figure 5.5 that θ ranges from $[-\pi, \pi]$ and thus it is also not possible to tell from with sector is the signal actually arriving since the only information that the system has is $\cos(\theta)$. The end result is that each sensor possesses two estimated lines in the ground plane where the transmitting node may be located. However, by acquiring a set of line estimates it is possible to obtain a single estimate of the transmitting sensor localization. Figure 5.6 shows an example of imprecise estimates from three receiving nodes being used to estimate the position of

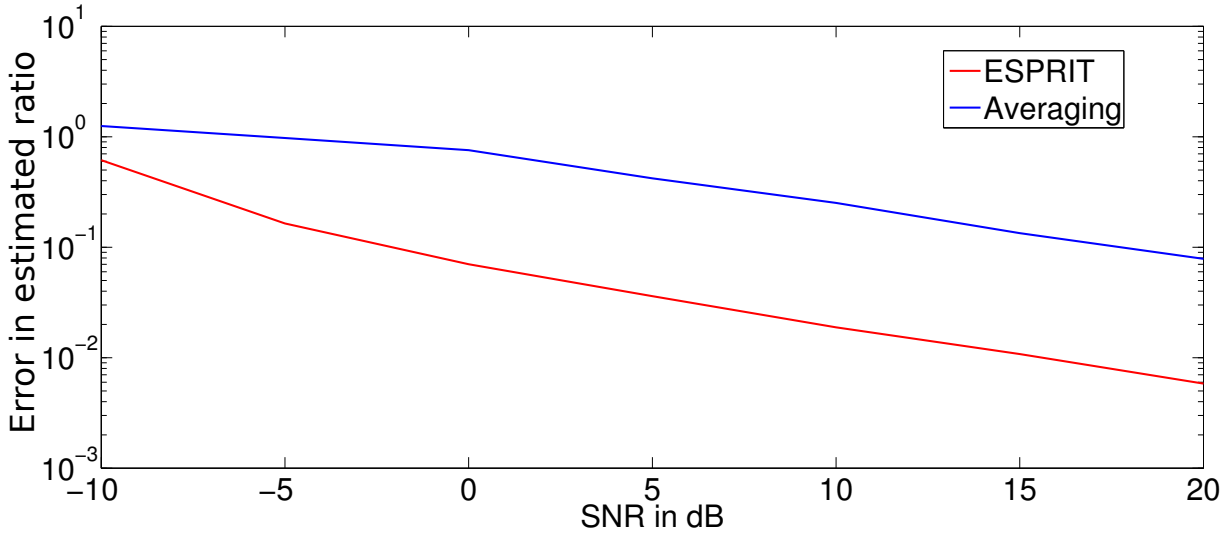

Figure 5.4: Comparison between ESPRIT and averaging samples

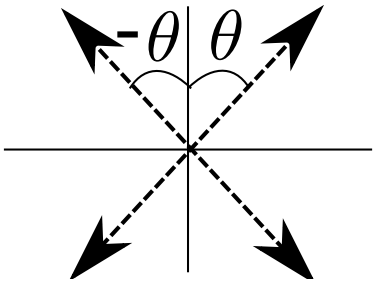

Figure 5.5: Depiction of possible ambiguity in signal propagation direction

the transmitter node. The problem is reduced to the least squares problem of finding the point with minimum distance from any of the possible combination of line estimates.

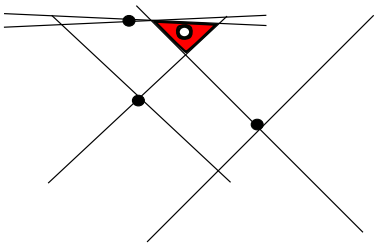

Figure 5.6: Sensor triangulation example

By writing the representing the line estimates as line equations of the type $Ax + By + C = 0$ in the sensor coordinate system, the estimate of the sensor position can be found by solving

$$\min_{p} \frac{|A_{p_1}x_0 + B_{p_1}y_0 + C_{p_1}|}{\sqrt{A_{p_1} + B_{p_1}}} + \frac{|A_{p_2}x_0 + B_{p_2}y_0 + C_{p_2}|}{\sqrt{A_{p_2} + B_{p_2}}} + ..., \tag{5.20}$$

where p is an index set containing the possible combinations of estimated lines. While more than three sensors can be used to obtain increased accuracy it also results in a higher computational load involved in the calculation of the minima. Once the lines are choose the final location estimate

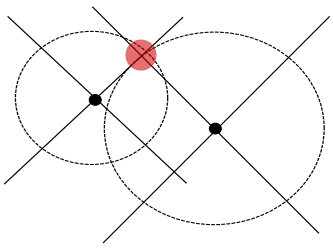

Figure 5.7: Sensor triangulation with RSSI information

$S_0 = [x_0, y_0]$ can be found by taking the derivative of the above with respect to x_0 and y_0 and finding the point where it is equal to zero.

Furthermore, this technique may be used in conjunction with other localization methods such as the RSSI. A set of candidate locations can be selected and the RSSI information can be used to choose the candidate that best fits the RSSI information as shown in Figure 5.7.

The whole localization of the entire network can be achieve as the individual sensor localizations are spread across the network.

5.2.4 Results and Discussion

The first result analyzed is how the precision of the estimated location is affected by the SNR of the transmitted signal. For this simulation the transmitting node is centered around three receiving nodes. The distance between the transmitting node and the receiving nodes is 100 m. 50 snapshots are used for the ratio estimation and booth the averaging and the ESPRIT methods are compared. The scenario is detailed in Figure 5.8.

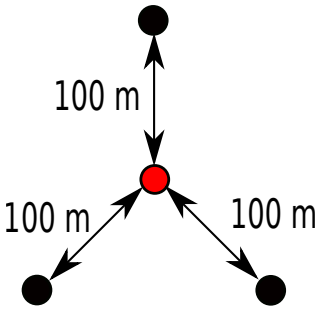

Figure 5.8: Illustration of first simulation scenario

The results shown in Figure 5.9 show how the error is affected by both the SNR and the selection of estimation method. Even for negative SNRs the ESPRIT method is capable of keeping the estimation error bellow 1 m. However, this scenario offers the advantage of a transmitting node centered in relation to the receiving nodes, thus, errors in angle estimation at each receiving node are more likely to end up compensating for each other.

To better analyze how the proposed method behaves in harsher scenario, more likely to be present in situations where the sensors are randomly placed in an area we place the receiving

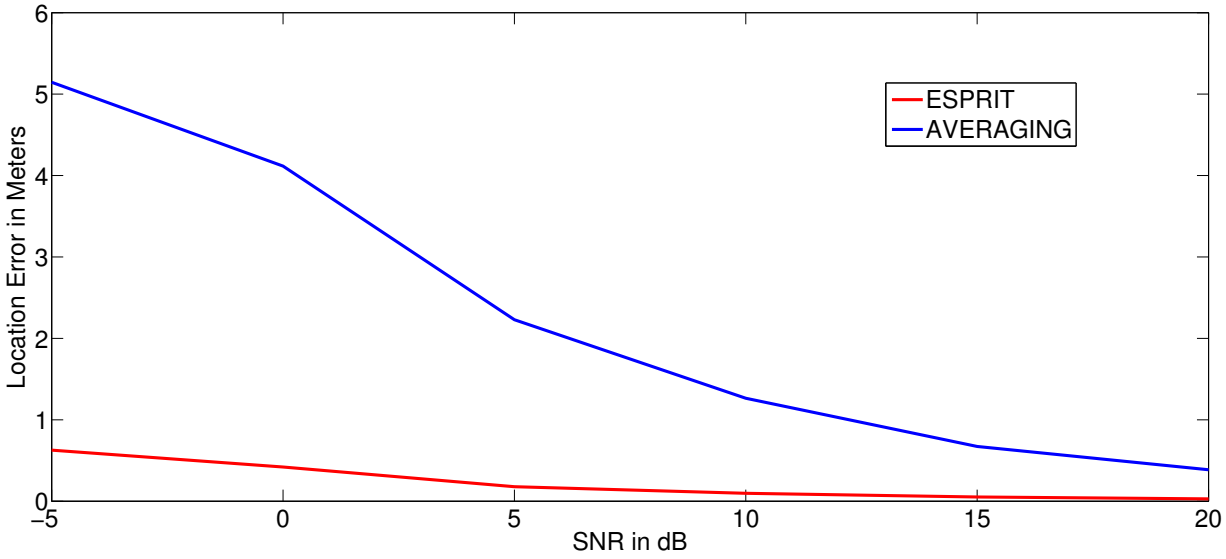

Figure 5.9: Location error for the first scenario

sensors in a single sector when the transmitted sensor is considered as the origin. Figure 5.10 presents graphically how the sensors were placed for the simulation.

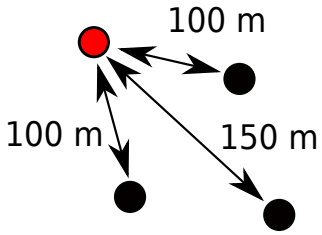

Figure 5.10: Illustration of second simulation scenario

Figure 5.11 shows how the error is affected not only by the SNR but also by the position of the receiving sensors. Since all sensors are located whiting a single sector with respect to the transmitting sensor the angle estimation errors result in a larger positioning error, since the estimated intersection or near intersection of the lines is more likely to be displaced by larger distances.

Finally to analyze the behavior of the proposed technique in an entire network environment and area of 1×1 km is filled with enough sensors to guarantee that every sensor has a neighbor within 150 m with probability 0.98. The number of nodes can be calculated using the formula

$$P = (1 - \mathrm{e}^{-d\pi r^2})^n,$$

where d is the sensor density in the area, r is the range at with the probability is to be calculated and n is the number of sensors deployed. In this case the necessary number of sensors is 130.

Figure 5.12 shows the location error averaged across the entire network. Since the location errors propagate the end result is higher location errors than when only a single estimation is considered. However, for high SNRs it is possible to notice that estimations within a 5 m errors

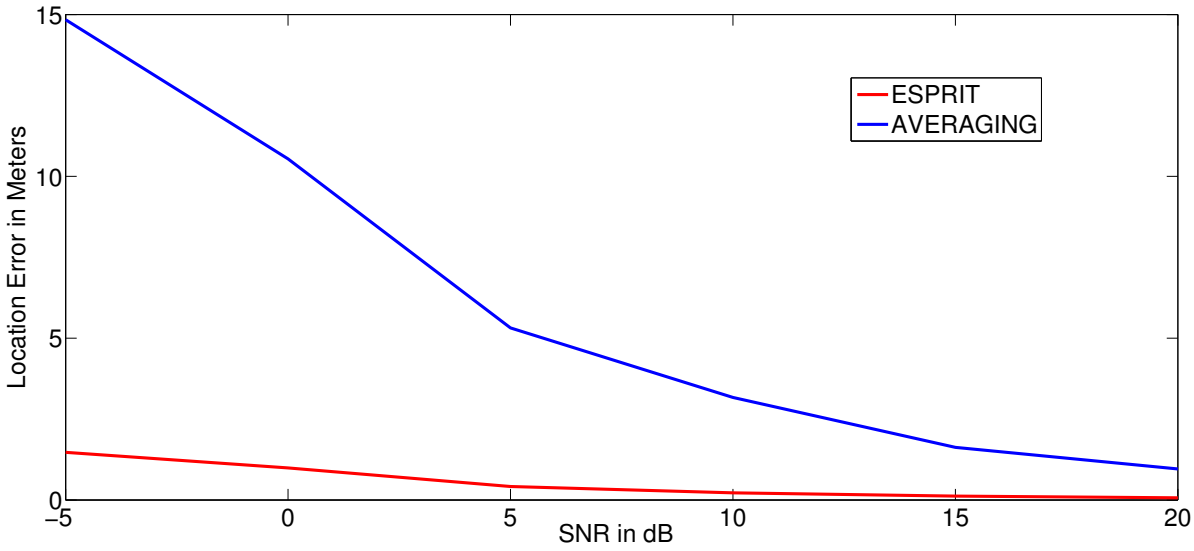

Figure 5.11: Location error for the second scenario

margin are achievable with the averaging method and withing a 2 m margin when employing the the ESPRIT method.

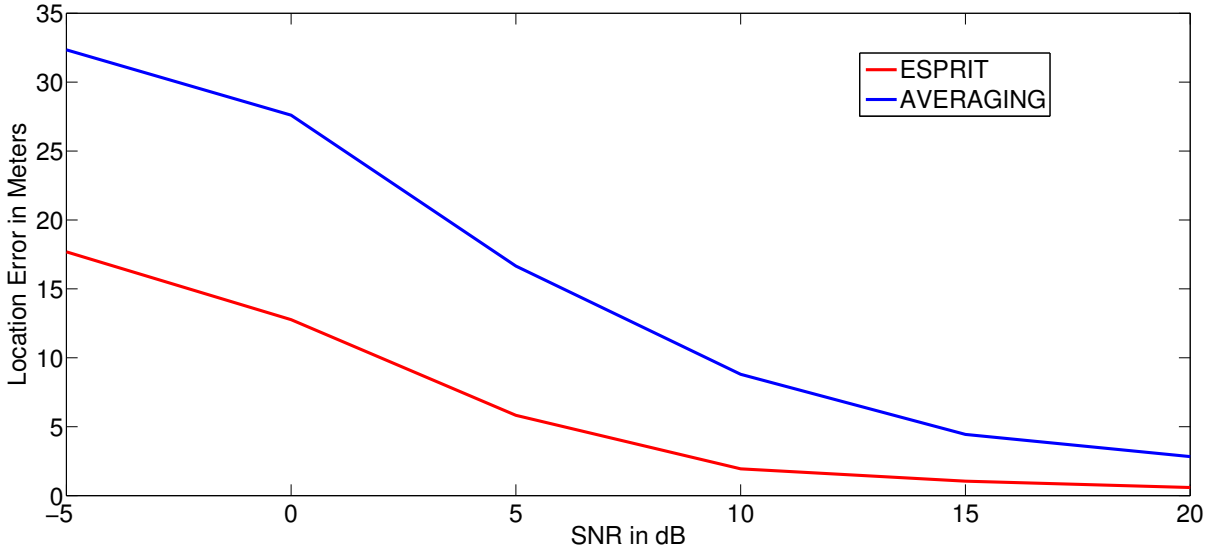

Figure 5.12: Location error for full network

5.2.5 Forming Virtual Antenna Arrays

Once the relative position of the sensors has been estimated a virtual antenna array can be formed. According to (3.3) the steering matrix for the entire sensor network can be constructed. By applying the approach proposed in Chapter 4 this arbitrary sensor network array can be interpolated into any kind of desired array, allowing the sensor network, for instance, to fight outside unfriendly jamming by performing spatial filtering, or allowing the sensor network to use

beamforming to transmit radio signals that would reach a much larger distance than normally.

5.3 Summary

In this chapter we presented two different applications of the interpolation technique proposed in Chapter 4. The first application was allowing arbitrary antenna arrays to be used to improve the performance of GNSS systems, getting rid of jamming, spoofing and multipath components. The entire framework for estimating the TDOA between satellite and receiver using and antenna array was presented. The second application was transforming a WSN with randomly placed elements into a full antenna array. A framework for acquiring the initial relative sensor localization in the network was present, allowing the network to operate as antenna array of any type.

Chapter 6

Conclusion

In this work an extensive framework for applying array interpolation to map the response of arrays of arbitrary into responses of arrays with a desired very specific geometry was presented. The proposed approach was shown to be able to deal with highly correlated signals and to perform considerably better than the current state-of-the-art approach present in the literature. As examples of the flexibility of the proposed approach two different applications were presented on completely different fields, an antenna array GNSS receiver and using a randomly placed WSN as an antenna array.

The first part presents a very detailed description of the most complex data model used in this work, the GNSS data model. Although this description may be tedious for the some readers it is important for the full understanding of all the work present here. Furthermore, it is the personal opinion of this author that the GNSS literature is extremely lacking and thus, presenting this fully detailed data model may help future researchers interested in this field to get acquainted with the details and nuances of the GNSS signals, as they differ heavily from the model often used in array signal processing data models.

The second part presents the main contribution of this work, a complete and novel framework for array interpolation. Prior works on array interpolation present on the literature use a sector-by-sector processing, where different transformation matrices are calculated for different regions of the field of view of the array without taking into account the received signal. Although this matrices can be calculated "off-line" since they only rely on the knowledge of the true array response they require that for each sector a DOA estimation step is performed. This leads to problems unanswered in the literature. The first problem is how to estimate the number of signals, using model order selection methods after transforming a sector may lead to highly imprecise results since nothing can be said of signals left outside of the transformed sector, the outside region of the transform is treated as a "don't care" region. The second step is how to choose between different estimates and decide whether they are estimates from the same signal or from different closely space signals. Since the transform does not care about signals outside of the sector it is possible that estimates for such signals still appear, how to select the best estimate if for each sector all signals appear in the final estimates? Even for works where the out-of-sector response is suppressed the suppression

is usually not enough to fully remove the statistics of the out-of-sector signals from the data, and even when enough, this suppression comes at the cost of a very high transformation error leading to very poor final estimates. This problems are not addressed in the current available literature and are extremely relevant for the application of array interpolation in real systems. In this work we propose a data adaptive array interpolation approach, the approach constructs a single transformation matrix that addresses all the regions of the field of view where significant power is arriving. This single transformation matrix is used to transform the data and allow the application of FBA and SPS when necessary, since no signal has been treated as a "don't care" a model order estimation method can be used to precisely estimate the number of incoming signals. The single transformation matrix also allows the application of the ESPRIT algorithm, applying ESPRIT with SPS and FBA in interpolated arrays is unheard of in the literature, to jointly estimate the DOAs of all signals fully eliminating the problem of selecting between different DOA estimates. The results of the proposed approach are compared with the currently state-of-the-art technique and are shown to achieve improved results. The results were also shown to be robust to a true model mismatch.

Finally, the third part presents different applications of the proposed array interpolation technique to prove is flexibility and applicability in real life problems. The first application is a antenna array based GNSS receiver, the array interpolation is used to allow the decorrelation of the highly correlated signals present in the GNSS environment in the form of multipath components, jamming or spoofing. A full framework for an antenna array GNSS receiver is presented with all the steps necessary for operating with a GNSS signal being detailed. An extension of the MUSIC algorithm usually used for DOA estimation is presented to estimate the TDOA instead. The second application is transforming a WSN with randomly placed elements into a fully functional antenna array. A full framework of sensor localization was presented, with the relative locations at hand, turning a WSN into a antenna array of any kind can be done by employing the proposed interpolation approach.

The interpolation approach proposed in this work can be further extended for any application that relies on sensor arrays of any kind, microphone arrays, light sensor arrays, etc. The proposed approach is also very relevant for real array implementations, extremely precise sensor positioning is not always possible, for example, placing an antenna array inside a cellphone would have serious space and placement restrictions. Even when the precise placement is possible the usual assumption of perfect omnidirectional and linear antennas does not hold true in reality, the proposed approach can be used to correct such imprecisions.

Array interpolation is still in its initial stage of study and further study is planed to achieve better transformation matrices that can deal better with true model mismatches or that can even operate blindly with respect to the true array response. Applying different regression models to the calculation of the transform matrix is also planned.

OWN PUBLICATIONS

[1*] E. P. Freitas, J. P. C. L. Costa, A. L. F. Almeida, and M. A. M. Marinho, "Applying MIMO techniques to minimize energy consumption for long distances communications in wireless sensor networks," in *NEW2AN/ruSMART 2012*, 2012.

[2*] M. A. M. Marinho, E. P. de Freitas, J. P. C. L. da Costa, A. L. F. de Almeida, and R. T. de Sousa Jr., "Using cooperative MIMO techniques and UAV relay networks to support connectivity in sparse wireless sensor networks," in *IEEE International Conference on Computing, Management and Telecommunications (ComManTEL)*, 2013.

[3*] M. A. M. Marinho, E. P. de Freitas, J. P. C. L. da Costa, A. L. F. de Almeida, and R. T. de Sousa Jr., "Using MIMO techniques to enhance communication among static and mobile nodes in wireless sensor networks," in *27th IEEE International Conference on Advanced Information Networking and Applications (AINA-2013)*, 2013.

[4*] R. S. Ferreira Júnior, M. A. M. Marinho, K. Liu, J. P. C. L. da Costa, A. V. Amaral, and H. C. So, "Improved landing radio altimeter for unmanned aerial vehicles based on an antenna array," in *IEEE IV International Conference on Ultra Modern Telecommunications and Control Systems (ICUMT)*, 2012, best paper award.

[5*] M. A. M. Marinho, R. S. Ferreira Júnior, J. P. C. L. da Costa, E. P. de Freitas, K. Liu, A. A. H. Cheung, R. T. de Sousa Jr., and R. Zelenovsky, "Antenna array based positioning scheme for unmanned aerial vehicles," in *17th International ITG Workshop on Smart Antennas (WSA 2013), 2013.*

[6*] Marinho, M. A. M. ; Antreich, F. ; Costa, J. P. C. L. . Improved Array Interpolation for Reduced Bias in DOA Estimation for GNSS. In: *ION ITM 2014, 2013, San Diego. ION ITM 2014, Procedings, 2014.*

[7*] Marinho, M. A. M. ; Freitas, E. P. ; Costa, J. P. C. L. ; Souza Junior, R. T. . Synchronization for Cooperative MIMO in Wireless Sensor Networks. In: *13th International Conference, NEW2AN 2013 and 6th Conference, ruSMART 2013, 2013, St. Petersburg. Internet of Things, Smart Spaces, and Next Generation Networking. Berlin: Springer Berlin Heidelberg, 2013. p. 298-311.*

[8*] Marinho, M. A. M. ; Freitas, E. P. ; Costa, J. P. C. L. ; Souza Junior, R. T. . Applying Cooperative MIMO Technique in an Adaptive Routing Mechanism for Wireless Sensor Net-

works. In: 2013 IEEE Conference on Wireless Sensors (ICWiSe2013), 2013, Sarawak. 2013 IEEE Conference on Wireless Sensors (ICWiSe2013), Proceedings, 2013

[9*] M. A. M. Marinho, F. Antreich, J. P. C. L. da Costa, J. Nossek, "Reduced Rank TLS Array Interpolation for DOA Estimation" in *17th International ITG Workshop on Smart Antennas (WSA 2013), 2013.*

[10*] R. S. Ferreira Júnior, M. A. M. Marinho, J. P. C. L. da Costa, A. V. Amaral, and R. T. de Sousa Jr., "Rádio Altímetro baseado em Arranjo de Antenas," Processo Nº.: BR 10 2013 002620 4, INPI.

REFERENCES

[1] R. S. F. Júnior, M. A. M. Marinho, K. Liu, J. P. C. L. da Costa, A. V. Amaral, and H. C. So, "Improved landing radio altimeter for unmanned aerial vehicles based on an antenna array," 2012.

[2] M. A. M. Marinho, R. S. F. Junior, J. P. C. L. da Costa, E. P. de Freitas, K. Liu, H. C. So, and F. Antreich, "Antenna array based positioning scheme for unmanned aerial vehicles," 2013.

[3] B. Ottersten, M. Viberg, and T. Kailath, "Analysis of Subspace Fitting and ML Techniques for Parameter Estimation from Sensor Array Data," *IEEE Transactions on Signal Processing*, vol. 40, no. 3, March 1992.

[4] B. Ottersten, M. Viberg, P. Stoica, and A. Nehorai, "Exact and large sample ML, techniques for parameter estimation and detection in array processing," *RadarArray Processing*, pp. 99–151.

[5] A. P. Dempster, N. M. Laird, and D. B. Rubin, "Maximum Likelihood from Incomplete Data via the EM Algorithm," *J. Royal Statistical Soc. B.*, vol. 39, no. 1, 1977.

[6] T. K. Moon, "The Expectation-Maximization Algorithm," *IEEE Signal Processing Magazine*, November 1996.

[7] G. J. McLachlan and T. Krishnan, *The EM Algorithm and Extensions.* John Wiley & Sons, Inc., New York, 1997.

[8] M. Miller and D. Fuhrmann, "Maximum-Likelhood Narrow-Band Direction Finding and the EM Algorithm," *IEEE Transactions on Acoustics Speech and Signal Processing*, vol. 38, pp. 1560–1577, 1990.

[9] J. A. Fessler and A. O. Hero, "Space-Alternating Generalized Expectation-Maximization Algorithm," *IEEE Transactions on Signal Processing*, vol. 42, no. 10, October 1994.

[10] F. A. Dietrich, "A Tutorial on Channel Estimation with SAGE," *Technical Report TUM-LNS-TR-06-03*, 2006.

[11] P. J. Chung and J. F. Bšohme, "Comparative convergence analysis of EM and SAGE algorithms in DOA estimation," *IEEE Transactions on Signal Processing*, vol. 49, pp. 2940–2949, 2001.

[12] M. Bartlett, "Smoothing Periodograms from Time Series with Continuous Spectra," *Nature*, vol. 161, pp. 686–687, 1948.

[13] J. Capon, "High-Resolution Frequency-Wavenumber Spectrum Analysis," *Proceedings IEEE*, vol. 57, pp. 1408–1418, 1969.

[14] J. E. Evans, J. R. Johnson, and D. F. Sun, "Application of advanced signal processing techniques to angle of arrival estimation in ATC navigation and surveillance system," Massachusetts Institute of Technology, Tech. Rep., 1982.

[15] S. Pillai and B. H. Kwon, "Forward/backward Spatial Smoothing Techniques for Coherent Signal Identification ," *IEEE Transactions on Acoustics, Speech and Signal Processing*, vol. 37, pp. 8–9, January 1989.

[16] B. Friedlander and A. Weiss, "Direction finding using spatial smoothing with interpolated arrays," *Aerospace and Electronic Systems, IEEE Transactions on*, vol. 28, pp. 574–587, 1992.

[17] B. Friedlander, "The root-MUSIC algorithm for direction finding with interpolated arrays," *Signal Processing*, vol. 30, pp. 15–29, 1993.

[18] M. Pesavento, A. Gershman, and Z.-Q. Luo, "Robust array interpolation using second-order cone programming," *Signal Processing Letters*, vol. 9, pp. 8–11, 2002.

[19] M. Buhren, M. Pesavento, and J. F. Böhme, "Virtual array design for array interpolation using differential geometry," in *Acoustics, Speech, and Signal Processing, 2004. Proceedings. (ICASSP '04). IEEE International Conference on*, vol. 2, 2004.

[20] R. O. Schmidt, "Multiple emitter location and signal parameter estimation," *IEEE Transactions on Antennas and Propagation*, vol. 34, pp. 276–280, 1986.

[21] A. J. Barabell, "Improving the Resolution Performance of Eigenstructured Based Direction-Finding Algorithms," in *Proceedings of ICASSP 83*, 1983.

[22] R. Roy and T. Kailath, "ESPRIT - estimation of signal parameters via rotation invariance techniques," *IEEE Transactions on Acoustics Speech and Signal Processing*, vol. 17, 1989.

[23] B. Lau, G. Cook, and Y. Leung, "An improved array interpolation approach to DOA estimation in correlated signal environments," in *Acoustics, Speech, and Signal Processing, 2004. Proceedings. (ICASSP '04). IEEE International Conference on*, 2004.

[24] B. Lau, M. Viberg, and Y. Leung, "Data-adaptive array interpolation for DOA estimation in correlated signal environments," in *Acoustics, Speech, and Signal Processing, 2005. Proceedings. (ICASSP '05). IEEE International Conference on*, 2005.

[25] R. O. Schmidt, "Multiple Emitter Location and Signal Parameter Estimation," *IEEE Transactions on Antennas and Propagation*, vol. 34, no. 3, March 1986.

[26] Y. Bresler and A. Macovski, "Exact Maximum Likelihood Estimation of Superimposed Exponentials Signals in Noise," *IEEE ASSP Magazine*, vol. 34, pp. 1081–189, 1986.

[27] P. Stoica and A. Nehorai, "A Novel Eigenanalysis Method for Direction Estimation," in *Proceedings IEEE F.*, 1990.

[28] T. Bronez, "Sector interpolation of non-uniform arrays for efficient high resolution bearing estimation," in *Acoustics, Speech, and Signal Processing, 1988. ICASSP-88., 1988 International Conference on*, 1988.

[29] M. Buhren, M. Pesavento, and J. F. Bohme, "A new approach to array interpolation by generation of artificial shift invariances: interpolated ESPRIT," in *Acoustics, Speech, and Signal Processing, 2003. Proceedings. (ICASSP '03). 2003 IEEE International Conference on*, 2003.

[30] A. Weiss and M. Gavish, "The interpolated ESPRIT algorithm for direction finding," in *Electrical and Electronics Engineers in Israel, 1991. Proceedings., 17th Convention of*, 1991.

[31] T. Kurpjuhn, M. Ivrlac, and J. Nossek, "Vandermonde Invariance Transformation," in *Acoustics, Speech, and Signal Processing, 2001. Proceedings. (ICASSP '01). 2001 IEEE International Conference on*, 2001.

[32] H. Krim and M. Viberg, "Two decades of array signal processing research: the parametric approach," *IEEE Signal Processing Magazine*, vol. 13, pp. 67–94, 1996.

[33] H. Krim and J. Proakis, "Smoothed Eigenspace-Based Parameter Estimation," *Auromaticu, Special Issue on Statistical Signal Processing and Control*, 1994.

[34] N. Wiener, "Extrapolation, Interpolation and Smoothing of Stationary Time Series," *MIT Press*, 1949.

[35] J. Cozzens and M. Sousa, "Source Enumeration in a Correlated Signal Environment," *IEEE Transactions on Acoustics Speech and Signal Processing*, vol. 42, pp. 304–317, 1994.

[36] M. Wax and T. Kailath, "Detection of signals by information by information theoric criteria," *IEEE Transactions on Acoustics Speech and Signal Processing*, vol. 33, pp. 387–392, 1985.

[37] E. Radoi and A. Quinquis, "A new method for estimating the number of harmonic components in noise with application in high resolution radar," *EURASIP Journal on Applied Signal Processing*, pp. 1177–1188, 2004.

[38] J. P. C. L. da Costa, M. Haardt, F. Romer, and G. Del Galdo, "Enhanced model order estimation using higher-order arrays," *Conference Record of The Forty-First Asilomar Conference on Signals, Systems & Computers*, pp. 412–416, 2007.

[39] J. P. C. L. da Costa, F. Roemer, M. Haardt, and R. T. de Sousa Jr., "Multi-Dimensional Model Order Selection," *EURASIP Journal on Advances in Signal Processing*, vol. 26, 2011.

[40] G. C. Reinsel and R. P. Velu, *Multivariate Reduced-Rank Regression*, S.-V. N. York, Ed. Springer New York, 1998.

[41] J. P. C. L. da Costa, D. Schulz, F. Roemer, M. Haardt, and J. A. A. Jr., "Robust R-D Parameter Estimation via Closed-Form PARAFAC in Kronecker Colored Environments," in *Proc. 7-th International Symposium on Wireless Communications Systems (ISWCS 2010)*, 2010.

[42] J. P. C. L. da Costa, F. Roemer, M. Weis, and M. Haard, "Robust R-D parameter estimation via closed-form PARAFAC," in *Proc. ITG Workshop on Smart Antennas (WSA'10)*, 2010.

[43] J. P. C. L. da Costa, S. Schwarz, L. F. de A. Gadêlha, H. C. Moura, G. A. Borges, and L. A. R. Pinheiromari, "Attitude determination for unmanned aerial vehicles via an antenna array," in *Proc. ITG IEEE Workshop on Smart Antennas (WSA12)*, Dresden Germany, March 2012.

[44] G. L. Sitzmann and G. H. Drescher, "Tactical ballistic missiles trajectory state and error covariance propagation," in *IEEE Position Location and Navigation Symposium.* Las Vegas, NV, USA: IEEE, April 1994, pp. 839–844.

[45] I. Akyildiz, W. Su, Y. Sankarasubramaniam, and E. Cayirci, "Wireless sensor networks: a survey," *Computer Networks*, vol. 38, pp. 393–422, 2002.

[46] K. Cheung, H. So, W. Ma, and Y. Chan, "Received Signal Strength Based Mobile Positioning via Constrained Weighted Least Squares," in *Proc. of Int. Conf. on Acoustics, Speech, and Signal Processing (ICASSP 2003)*, 2003.

[47] R. Nagpal, H. Shrobe, and J. Bachrach, "Organizing a global coordinate system from local information on an ad hoc sensor network," in *IPSN*, 2003.

[48] R. Biswas and S. Thrun, "A passive approach to sensor network localization," in *Intelligent Robots and Systems, 2004. (IROS 2004). Proceedings. 2004 IEEE/RSJ International Conference on*, 2004.

[49] J. Li and J. Compton, R.T., "Angle and polarization estimation using ESPRIT with a polarization sensitive array," *Antennas and Propagation, IEEE Transactions on*, vol. 39, pp. 1376 – 1383, 1991.

Appendix A

Forward Backward Averaging and Spatial Smoothing

In this work, since we consider highly correlated signals. Forward Backward Averaging and Spatial Smoothing are of paramount importance. In this section these techniques are detailed and its effect in a possible rank deficient signal correlation matrix is shown. Both these techniques require a regular array geometry such as a ULA or URA as mentioned, this can be virtually obtained via array interpolation as shown in this work. The Forward Backward Averaged received signal matrix is constructed as

$$\mathbf{Z} = [\mathbf{X}|\mathbf{Q}_M\mathbf{X}^*\mathbf{Q}_N], \tag{A.1}$$

where $\mathbf{Q}_n$ is a $n \times n$ exchange matrix given in (4.1). Let $\mathbf{A}$ be a steering matrix for $d = 3$ and $M = 3$ in a centro-hermitian array

$$\mathbf{A} = \begin{bmatrix} \mathrm{e}^{-\mathrm{j}\mu_1} & \mathrm{e}^{-\mathrm{j}\mu_2} & \mathrm{e}^{-\mathrm{j}\mu_3} \\ 1 & 1 & 1 \\ \mathrm{e}^{\mathrm{j}\mu_1} & \mathrm{e}^{\mathrm{j}\mu_2} & \mathrm{e}^{\mathrm{j}\mu_3} \end{bmatrix}. \tag{A.2}$$

Thus, we have

$$\mathbf{Q}_M\mathbf{A} = \begin{bmatrix} \mathrm{e}^{\mathrm{j}\mu_1} & \mathrm{e}^{\mathrm{j}\mu_2} & \mathrm{e}^{\mathrm{j}\mu_3} \\ 1 & 1 & 1 \\ \mathrm{e}^{-\mathrm{j}\mu_1} & \mathrm{e}^{-\mathrm{j}\mu_2} & \mathrm{e}^{-\mathrm{j}\mu_3} \end{bmatrix} \tag{A.3}$$

and

$$\mathbf{Q}_M\mathbf{A}^* = \begin{bmatrix} \mathrm{e}^{-\mathrm{j}\mu_1} & \mathrm{e}^{-\mathrm{j}\mu_2} & \mathrm{e}^{-\mathrm{j}\mu_3} \\ 1 & 1 & 1 \\ \mathrm{e}^{\mathrm{j}\mu_1} & \mathrm{e}^{\mathrm{j}\mu_2} & \mathrm{e}^{-\mathrm{j}\mu_3} \end{bmatrix}. \tag{A.4}$$

The signal matrix for $N = 3$ can be written as

$$\mathbf{S} = \begin{bmatrix} s_{1,1} & s_{1,2} & s_{1,3} \\ s_{2,1} & s_{2,2} & s_{2,3} \\ s_{3,1} & s_{3,2} & s_{1,3} \end{bmatrix}, \tag{A.5}$$

and

$$\mathbf{SQ}_N^* = \begin{bmatrix} s_{1,1}^* & s_{1,2}^* & s_{1,3}^* \\ s_{2,3}^* & s_{2,2}^* & s_{2,1}^* \\ s_{3,3}^* & s_{3,2}^* & s_{3,1}^* \end{bmatrix}. \tag{A.6}$$

The steering matrix is not affected by the transformation, i.e., the DOAs of the normal and Forward Backward Averaged version are the same, therefore $\mathbf{X}$ and $\mathbf{Q}_M\mathbf{X}^*\mathbf{Q}_N$ can be concatenated. Also, $\mathbf{SQ}_N^*$ virtually enhances the number of samples to a degree that depends on the correlation between the incoming signals, as shown latter in the appendix. In the case when only noise is present we have

$$\mathbf{Z} = \begin{bmatrix} n_{1,1} & n_{1,2} & n_{1,3} & n_{1,3}^* & n_{1,2}^* & n_{1,1}^* \\ n_{2,1} & n_{2,2} & n_{2,3} & n_{2,3}^* & n_{2,2}^* & n_{2,1}^* \\ n_{3,1} & n_{3,2} & n_{3,3} & n_{3,3}^* & n_{3,2}^* & n_{3,1}^* \end{bmatrix}, \tag{A.7}$$

since the entries $n_{i,j}$ are drawn from $\mathcal{CN}(0, \sigma_n^2)$ the noise samples are spatially uncorrelated.

A similar analysis can be made for Spatial Smoothing dividing the array into two subarrays of length $L = 2$. The steering matrices are

$$\mathbf{A}^{(1)} = \begin{bmatrix} \mathrm{e}^{-\mathrm{j}\mu_1} & \mathrm{e}^{-\mathrm{j}\mu_2} & \mathrm{e}^{-\mathrm{j}\mu_3} \\ 1 & 1 & 1 \end{bmatrix}, \tag{A.8}$$

$$\mathbf{A}^{(2)} = \begin{bmatrix} 1 & 1 & 1 \\ \mathrm{e}^{\mathrm{j}\mu_1} & \mathrm{e}^{\mathrm{j}\mu_2} & \mathrm{e}^{\mathrm{j}\mu_3} \end{bmatrix}. \tag{A.9}$$

Therefore, $\mathbf{A}^{(1)}$ and $\mathbf{A}^{(2)}$ introduce the same phase delay between the signal samples and can be used to obtain two independent DOA estimations from

$$\mathbf{A}^{(1)}\mathbf{S}, \tag{A.10}$$

$$\mathbf{A}^{(2)}\mathbf{S}, \tag{A.11}$$

at the price of sacrificing an antenna for each estimation. These estimations can be, for simplicity, averaged uniformly.

A deeper analysis can be made by looking into the effects on the covariance of the received signal. We define

$$\mathbf{D} = \mathrm{diag}[\mathrm{e}^{\mathrm{j}\theta_1}, \mathrm{e}^{\mathrm{j}\theta_2}, ..., \mathrm{e}^{\mathrm{j}\theta_d}]. \tag{A.12}$$

The covariance matrix of the signal received at the $i-$th subarray of length W can be written as

$$\mathbf{R}\mathbf{X}\mathbf{X}_W^{(i)} = \mathbf{A}_W\mathbf{D}^{\frac{W-M}{2}+(i-1)}\mathbf{R}_{\mathbf{SS}}[\mathbf{D}^{\frac{W-M}{2}+(i-1)}]^{\mathrm{H}}\mathbf{A}_W^{\mathrm{H}} + \sigma_n^2\mathbf{I}. \tag{A.13}$$

The backward covariance matrix of the $i-$th subarray is given by $\mathbf{R}\mathbf{X}\mathbf{X}_{WB}^{(i)} = \mathbf{Q}[\mathbf{R}\mathbf{X}\mathbf{X}_W^{(i)}]^*\mathbf{Q}$,where $\mathbf{Q}$ is the exchange matrix given in (4.1). Given that $\mathbf{Q}\mathbf{A}_W^* = \mathbf{A}_W$ the backward signal covariance matrix is given by

$$\mathbf{R}\mathbf{X}\mathbf{X}_{WB}^{(i)} = \mathbf{A}_W[\mathbf{D}^{\frac{W-M}{2}+(i-1)}]^*[\mathbf{R}_{\mathbf{SS}}]^*[\mathbf{D}^{\frac{W-M}{2}+(i-1)}]^{*\mathrm{H}}\mathbf{A}_M^{\mathrm{H}} + \sigma_n^2\mathbf{I}. \tag{A.14}$$

By performing a uniform weighting across the subarrays we obtain the total covariance matrix

$$\mathbf{R_{XX}}_{SSFB} = \frac{1}{2L}\sum_{i=1}^{L}(\mathbf{R_{XX}}_{W}^{(i)} + \mathbf{R_{XX}}_{WB}^{(i)}), \tag{A.15}$$

where L is the total number of subarrays employed. Since $\mathbf{D}^* = \mathbf{D}^{-1}$ we can write

$$\begin{aligned}\mathbf{R_{XX}}_{SSFB} &= \mathbf{A}_W[\frac{1}{2L}\sum_{i=1}^{L}\mathbf{D}^{\frac{W-M}{2}+(i-1)}\mathbf{R_{SS}}[\mathbf{D}^{\frac{W-M}{2}+(i-1)}]^{\mathrm{H}} \\ &\quad +[\mathbf{D}^{\frac{W-M}{2}+(i-1)}]^*[\mathbf{R_{SS}}]^*[\mathbf{D}^{\frac{W-M}{2}+(i-1)}]^{*\mathrm{H}}]\mathbf{A}_W^{\mathrm{H}} + \sigma_n^2\mathbf{I}.\end{aligned} \tag{A.16}$$

The smoothed signal covariance can be rewritten as

$$\begin{aligned}\mathbf{R_{SS}}_{SSFB} &= \frac{1}{2L}\sum_{i=1}^{L}\mathbf{D}^{\frac{W-M}{2}+(i-1)}\mathbf{R_{SS}}[\mathbf{D}^{\frac{W-M}{2}+(i-1)}]^{\mathrm{H}} \\ &\quad +[\mathbf{D}^{\frac{W-M}{2}+(i-1)}]^*[\mathbf{R_{SS}}]^*[\mathbf{D}^{\frac{W-M}{2}+(i-1)}]^{*\mathrm{H}} \\ &= \frac{1}{L}\sum_{i=1}^{L}\mathrm{Re}[\mathbf{D}^{\frac{W-M}{2}+(i-1)}\mathbf{R_{SS}}[\mathbf{D}^{\frac{W-M}{2}+(i-1)}]^{\mathrm{H}}].\end{aligned} \tag{A.17}$$

Thus, if the cross correlation between the signals is a purely imaginary number it is completely mitigated by the Forward Backward averaging alone. Considering that only spatial smoothing was applied we have that its elements are given by

$$[\mathbf{R_{SS}}_{SS}^{(L)}]_{ij} = [\mathbf{R_{SS}}]_{ij}\frac{1}{L}\sum_{l-1}^{L}\mathbf{D}_{ii}^{\frac{W-M}{2}+(l-1)}[\mathbf{D}_{jj}^{\frac{W-M}{2}+(l-1)}]^*. \tag{A.18}$$

When $i = j$

$$[\mathbf{R_{SS}}_{SS}^{(L)}]_{ij} = [\mathbf{R_{SS}}]_{ii}, \tag{A.19}$$

when $i \neq j$ we have

$$\begin{aligned}\frac{1}{L}\sum_{l=1}^{L}\mathbf{D}_{ii}^{\frac{W-M}{2}+(l-1)}[\mathbf{D}_{jj}^{\frac{W-M}{2}+(l-1)}]^* &= \frac{1}{L}\sum_{l=1}^{L}\mathrm{e}^{\mathrm{j}\frac{\mathrm{W-M}}{2}(\theta_\mathrm{i}-\theta_\mathrm{j})}\mathrm{e}^{-\mathrm{j}(l-1)(\theta_i-\theta_j)} \\ &= \mathrm{e}^{\mathrm{j}\frac{\mathrm{W-M}}{2}\Delta\theta_\mathrm{ij}}\frac{1}{L}\sum_{m-1}^{L-1}\mathrm{e}^{\mathrm{j}m\Delta\theta_{ij}}.\end{aligned} \tag{A.20}$$

Thus, the effectiveness of Spatial Smoothing depends directly on the difference between the $\Delta\theta_{ij}$ between the angles of arrival of the signals indexed by i and j, this is why Spatial Smoothing is applied mostly in a heuristic manner and why, in this work, a simple way of choosing the minimum number of subarrays that provides proper signal decorrelation was proposed.